estimated to be ~16% by SSCP analysis. The PamChip microarray could detect mutant alleles proportions >25% by SSCP analysis. The limit for detection of mutant alleles by the PamChip microarray was therefore estimated to be 16–25% of the total DNA. The detection limit of direct sequencing was estimated to be 46–50%.

Discussion

In this study, we analyzed several mixtures containing two oligonucleotides (wild-type plus mutant) with the PamChip microarray. We also analyzed mixtures of genomic DNA (wild-type and mutant) prepared from two cell lines with the PamChip microarray. The fluorescence intensities of each sequence showed dose-dependent relationships and were somewhat consistent with the theoretical proportions in the mixtures of genomic DNA as well as oligonucleotides. Such results for microarray analysis have not been described previously. The accuracy of the fluorescence intensity and the degree of fluorescence were satisfactory and are suitable for microarray analysis.

Clinical DNA samples were analyzed with the PamChip microarray for comparison with PCR-SSCP analysis and/or DNA sequencing data. When somatic mutations in cancer tissues are assessed, it is not possible to avoid contamination by the wild-type allele derived from noncancer cells. We therefore investigated the limit at which each technique could detect the mutant allele. The ability to detect small amounts of mutant DNA within a large amount of wild-type DNA is absolutely necessary for analyzing clinical DNA samples. The combination of PCR-SSCP analysis and DNA sequencing provided the greatest sensitivity. Direct sequencing of PCR products occasionally misdiagnosed samples containing low amounts of the mutant allele (46–50%), and PCR-SSCP analysis could not distinguish genotypes with similar electrophoretic patterns. The PamChip microarray detected DNA mutations when the mutation comprised at least 25% of the tested population of DNA; thus, we believe that samples from patients heterozygous for a particular mutation, i.e., cancer specimens contaminated with noncancerous tissue, would be detectable with this array system. Mutations in mitochondrial DNAs that cause disease typically occur as mixtures of mutant and wild-type mitochondrial DNAs (heteroplasmy), and disease severity is correlated with the proportion of mutant DNA (*21*). Genotyping of mitochondrial DNA mutations in such diseases can also be performed with this array system.

The entire PamChip process was completed in ~3.25 h, including 1 h for DNA preparation, 2 h for PCR, and 15 min for microarray (hybridization, washing, and signal detection). The PamChip microarray thus substantially reduces the time necessary for microarray analysis. However, at present the PamChip microarray requires PCR amplification of the targeted region, which adds 2–3 h to the total analysis time. To reduce the time for DNA amplification, shuttle PCR or another amplification method may be useful. Multiplex PCR can be used to amplify multiple SNPs simultaneously. A novel microarray analysis that does not require DNA amplification or preparation would be superior for mutation and/or SNP analysis. Such a technique could be easily applied to the selection of medications best suited for each individual and to molecular diagnosis during surgery.

K-*ras* mutations are typically localized in codons 12, 13, and 61, and ~60% of somatic mutations in cancers occur in codon 12. Amino acid substitutions may affect the physiologic function of a protein and the clinical prognosis. A close association has been reported between a somatic mutation, GAT (Asp), in codon 12 and distant hematogenous metastasis (*22*). Two specific mutations, TGT (Cys) in codon 12 and GAC (Asp) in codon 13, have been associated with a significantly increased risk of cancer recurrence (*23*). Etiologic data revealed that GTT (Val) in codon 12 is associated with cancer progression and more aggressive biological behavior (*24, 25*). Consequently, genotyping of colorectal adenocarcinomas for K-*ras* status is feasible for use in diagnostic pathology to provide information that could be used to individualize and optimize treatments and prognoses.

In conclusion, the unique features of the PamChip microarray technology, including real-time imaging and temperature control combined with short assay time, make it suitable for clinical screening of mutations. This microarray is potentially useful for limited and targeted purposes, and detection of K-*ras* mutations is one example of such focused use of this microarray.

This research was supported in part by a Grant-in-Aid for Labour Sciences Research (H15-Cancer Prevention-9) for research on cancer prevention and health services; by a Grant-in-Aid from the Second Term Comprehensive 10-Year Strategy for Cancer Control from the Ministry of Health, Labour and Welfare, Japan; by a Grant-in-Aid for Scientific Research (B), for COE (Hamamatsu University School of Medicine); by a Grant-in-Aid from the Ministry of Education, Science, Sports, Culture and Technology, Japan; and by the Smoking Research Foundation.

References

1. Macgregor PF, Squire JA. Application of microarrays to the analysis of gene expression in cancer. Clin Chem 2002;48:1170–7.
2. Santacroce R, Ratti A, Caroli F, Foglieni B, Ferraris A, Cremonesi L, et al. Analysis of clinically relevant single-nucleotide polymorphisms by use of microelectronic array technology. Clin Chem 2002;48:2124–30.
3. Gentalen E, Chee M. A novel method for determining linkage between DNA sequences: hybridization to paired probe arrays. Nucleic Acids Res 1999;27:1485–91.
4. Huang JX, Mehrens D, Wiese R, Lee S, Tam SW, Daniel S, et al. High-throughput genomic and proteomic analysis using microarray technology. Clin Chem 2001;47:1912–6.

5. Frayling IM. Methods of molecular analysis: mutation detection in solid tumours. Mol Pathol 2002;55:73–9.
6. Hoque MO, Lee CC, Cairns P, Schoenberg M, Sidransky D. Genome-wide genetic characterization of bladder cancer: a comparison of high-density single-nucleotide polymorphism arrays and PCR-based microsatellite analysis. Cancer Res 2003;63:2216–22.
7. Wikman FP, Lu ML, Thykjaer T, Olesen SH, Andersen LD, Cordon-Cardo C, et al. Evaluation of the performance of a p53 sequencing microarray chip using 140 previously sequenced bladder tumor samples. Clin Chem 2000;46:1555–61.
8. Chizhikov V, Rasooly A, Chumakov K, Levy DD. Microarray analysis of microbial virulence factors. Appl Environ Microbiol 2001;67:3258–63.
9. Lucito R, Healy J, Alexander J, Reiner A, Esposito D, Chi M, et al. Representational oligonucleotide microarray analysis: a high-resolution method to detect genome copy number variation. Genome Res 2003;13:2291–305.
10. Foglieni B, Cremonesi L, Travi M, Ravani A, Giambona A, Rosatelli MC, et al. β-Thalassemia microelectronic chip: a fast and accurate method for mutation detection. Clin Chem 2004;50:73–9.
11. Cooper M, Li S-Q, Bhardwaj T, Rohan T, Kandel RA. Evaluation of oligonucleotide arrays for sequencing of the *p53* gene in DNA from formalin-fixed, paraffin-embedded breast cancer specimens. Clin Chem 2004;50:500–8.
12. Sassi AP, Paulus A, Cruzado ID, Bjornson T, Hooper HH. Rapid, parallel separations of d1S80 alleles in a plastic microchannel chip. J Chromatogr A 2000;894:203–17.
13. Sosnowski RG, Tu E, Butler WF, O'Connell JP, Heller MJ. Rapid determination of single base mismatch mutations in DNA hybrids by direct electric field control. Proc Natl Acad Sci U S A 1997;94:1119–23.
14. van Beumingen R, van Damme H, Boender P, Bastiaensen N, Chan A, Kievits T. Fast and specific hybridization using flow-through microarrays on porous metal oxide. Clin Chem 2001;47:1931–3.
15. Hokaiwado N, Asamoto M, Tsujimura K, Hirota T, Ichihara T, Satoh T, et al. Rapid analysis of gene expression changes caused by liver carcinogens and chemopreventive agents using a newly developed three-dimensional microarray system. Cancer Sci 2004;95:123–30.
16. Yanez L, Groffen J, Valenzuela DM. c-K-ras mutations in human carcinomas occur preferentially in codon 12. Oncogene 1987;1:315–8.
17. Maekawa M, Sugano K, Ushiama M, Fukayama N, Nomoto K, Kashiwabara H, et al. Heterogeneity of DNA methylation status analyzed by bisulfite-PCR-SSCP and correlation with clinico-pathological characteristics in colorectal cancer. Clin Chem Lab Med 2001;39:121–8.
18. Maekawa M, Taniguchi T, Tatebayashi C, Horii T, Takeshita A, Sugimura H, et al. Basic studies on mutation analysis of K-ras codon 12 by use of three-dimensional microarray system. Rinsho Byori 2003;51:306–12.
19. Verlaan-de Vries M, Bogaard ME, van den Elst H, van Boom JH, van der Eb AJ, Bos JL. A dot-blot screening procedure for mutated ras oncogenes using synthetic oligodeoxynucleotides. Gene 1986;50:313–20.
20. Sugano K, Kyogoku A, Fukayama N, Ohkura H, Shimosato Y, Sekiya T, et al. Methods in laboratory investigation. Rapid and simple detection of c-Ki-ras2 gene codon 12 mutations by nonradioisotopic single-strand conformation polymorphism analysis. Lab Invest 1993;68:361–6.
21. Wallace DC. Mitochondrial genetics: a paradigm for aging and degenerative diseases? Science 1992;256:628–32.
22. Finkelstein SD, Sayegh R, Christensen S, Swalsky PA. Genotypic classification of colorectal adenocarcinoma. Cancer 1993;71:3827–38.
23. Cerottini J-P, Caplin S, Saraga E, Givel J-C, Benhattar J. The type of K-ras mutation determines prognosis in colorectal cancer. Am J Surg 1998;175:198–202.
24. Al-Mulla F, Going JJ, Sowden ET, Winter A, Pickford IR, Birnie GD. Heterogeneity of mutant versus wild-type Ki-ras in primary and metastatic colorectal carcinomas, and association of codon-12 valine with early mortality. J Pathol 1998;185:130–8.
25. Andreyev HJ, Norman AR, Cunningham D, Oates J, Dix BR, Iacopetta BJ, et al. Kirsten ras mutations in patients with colorectal cancer: the 'RASCAL II' study. Br J Cancer 2001;85:692–6.

Lactate dehydrogenase (LD) extra isoenzyme electrophoretic band between LD1 and LD2 caused by a complex with α_1-lipoprotein. A case report

Jinko Ishikawa, Kiyotaka Fujita, Takashi Kanno and Masato Maekawa

Reprint
CLINICAL CHEMISTRY AND LABORATORY MEDICINE, No. 01/2004

Clin Chem Lab Med 2004;42(1):102–104 © 2004 by Walter de Gruyter • Berlin • New York

Letter to the Editor

Lactate dehydrogenase (LD) extra isoenzyme electrophoretic band between LD1 and LD2 caused by a complex with α_1-lipoprotein. A case report

Jinko Ishikawa[1], Kiyotaka Fujita[2], Takashi Kanno[1] and Masato Maekawa[1,*]

[1] Department of Laboratory Medicine, Hamamatsu University School of Medicine, Hamamatsu, Japan
[2] Department of Biomedical Laboratory Sciences, School of Health Sciences, Shinshu University, Matsumoto, Japan

Keywords: complex; isoenzyme; lactate dehydrogenase; α_1-lipoprotein.

There have been some reports of unusual lactate dehydrogenase (LD; EC 1.1.1.27) isoenzymes (1–12). An abnormal electrophoretic pattern may result from the presence of an extra LD fraction, altered mobility, a change in the molecular structure of a fraction or from the distortion of one or more normal bands (1). Distortion of normal bands may be caused by immunoglobulin (Ig) or any other protein binding (2–6), genetic variants (7, 8), tumor production (9, 10) and other modifications (11, 12). Complexes of LD and immunoglobulin are found in the sera of some patients (2–5), their presence usually indicated by electrophoretically abnormal LD fractions. Trocha (6) reported a case with seven LD isoenzyme bands in the serum assay and identified LD linked to β-lipoproteins and IgA. Baxi et al. (11) found an association between a surface antigen of hepatitis B virus and an LD isoenzyme that appeared as an anomalous band between LD4 and LD5 (LD5ex). Cabello et al. (12) described an additional band on the cathodic side of LD5 (namely LD6) having alcohol dehydrogenase activity.

An unusual extra electrophoretic band has also been observed in cancer patients (9, 10). The electrophoretic mobility of the extra band was often close to LD2 and between LD2 and LD3. We found that the extra band migrated slightly slower than LD2 in a patient with retinoblastoma, that the somatic *LDHA* gene was transcriptionally silenced by promoter hypermethylation of *LDHA* and that a testis-specific variant transcript of *LDHA* was related to the formation of the extra band (10).

*Corresponding author: Dr. Masato Maekawa, Department of Laboratory Medicine, Hamamatsu University School of Medicine, Handayama 1-20-1, Hamamatsu, 431-3192, Japan
Phone: +81-53-435-2721, Fax: +81-53-435-2794,
E-mail: mmaekawa@hama-med.ac.jp

We have discovered a patient with high serum LD activity and an extra electrophoretic band between LD1 and LD2. The patient was a 61-year-old woman with atypical mycobacterium infection and intermittent atrial arrhythmia. Values for some serum enzyme activities were aspartate aminotransferase, 37 IU/l (reference interval 11–30 IU/l); alanine aminotransferase, 19 IU/l (5–42 IU/l); creatine kinase, 94 IU/l (42–164 IU/l); and LD, 367 IU/l (101–193 IU/l). LD activity was measured by the method recommended by the Japanese Society for Clinical Chemistry (13) with a Hitachi 7350 biochemical automated analyzer (Hitachi, Ibaragi, Japan). The patient's LD activity in serum was elevated moderately.

The LD isoenzyme electrophoretic pattern in the patient's serum (lane 1) is shown in Figure 1A. We separated the isoenzymes by electrophoresis on a Titan III LIPO cellulose acetate film (Helena Laboratory, Saitama, Japan). An extra band between LD1 and LD2 was observed in several serum samples obtained on different days. There was no smearing pattern or broad banding pattern in any isoenzyme band. The proportions of LD1 (32.6%), the extra band (15.5%), LD2 (27.0%), LD3 (14.3%), LD4 (4.7%) and LD5 (6.0%) were determined from a densitometric trace. We also performed electrophoresis on a 4 to 20% gradient polyacrylamide gel (Multigel 4/20; Daiichi Pure Chemicals, Tokyo, Japan) and obtained two extra bands between LD2 and LD3 (Figure 1B). This means that the extra band obtained on cellulose acetate had a higher molecular mass than normal LD isoenzyme and that the extra band might have contained a complex between an LD isoenzyme and another protein.

To investigate whether the unusual protein was a genetic variant, we evaluated the LD isoenzyme pattern of erythrocyte hemolysates. Erythrocyte hemolysates were made as described previously (8) and used for LD isoenzyme analysis. If a genetic variant were present in the LD isoenzyme, the hemolysates should also yield the extra band, but none was obtained (data not shown).

Triton X-100 solution (10%) was added to the patient's serum to disrupt membrane bound molecules, and its effect on the LD isoenzyme pattern was determined. A substrate-blank reagent (without lactate, Helena Laboratory) was applied for LD staining instead of the usual staining solution to determine whether the extra band was LD. Neither treatment altered the amount of the extra band (data not shown).

We performed immunoelectrophoresis (IEP) using Titan Gel IE plates (Helena Laboratory) and antiserum

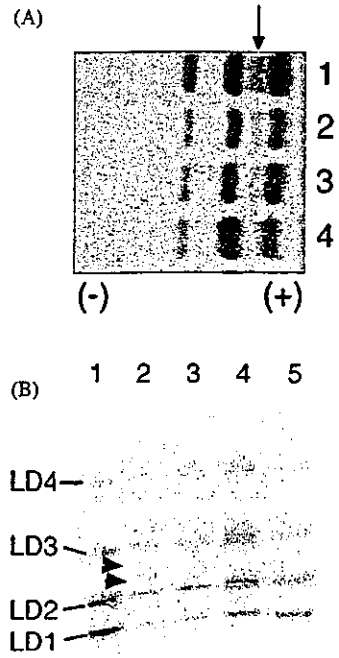

Figure 1 Abnormal lactate dehydrogenase (LD) isoenzyme pattern. A. Cellulose acetate membrane electrophoresis on a Titan III membrane. Lane 1, the patient's serum (PS) with the extra band marked by the arrow; lane 2, mixture of the PS and isotonic saline (1:6); lane 3, supernatant after mixing the PS with anti-α_2-macroglubulin antibody (1:6); lane 4, supernatant after mixing the PS with anti-α_1-lipoprotein antiserum (1:6). The extra band disappeared only in lane 4. The LD2 band in lane 4 is stronger than the LD1 band because of the LD activity in the antiserum (anti-α_1-lipoprotein). B. Gradient polyacrylamide (4–20%) gel electrophoresis. Lanes 1 and 5, LD1 and LD2 dominant control serum; lane 4, LD2 and LD3 dominant control serum; lanes 2 and 3, the PS sampled on different days 2 weeks apart. Two extra bands are marked by arrowheads.

against whole human serum (Helena Laboratory). Only one precipitin line was stained by LD activity in the α_1-globulin region (Figure 2). Based on the location and shape of the line, we suspected α_1-lipoprotein might be bound to LD. We then used antisera specific for α_1-lipoprotein (Daiichi Pure Chemicals), α_1-antitrypsin (Behring, Marburg, Germany) and α_1-acid glycoprotein (Behring). No LD activity was observed for any of the precipitin lines (data not shown). We also performed an immunoabsorption experiment. The patient's serum was mixed with the antiserum specific for α_1-lipoprotein and an antibody specific for α_2-macroglobulin (Dako, Glostrup, Denmark) for 30 min at 37°C, and the supernatant was analyzed for LD isoenzyme. The extra band disappeared when antiserum specific for α_1-lipoprotein, but not for α_2-macroglobulin, was applied (Figure 1A, lanes 3 and 4).

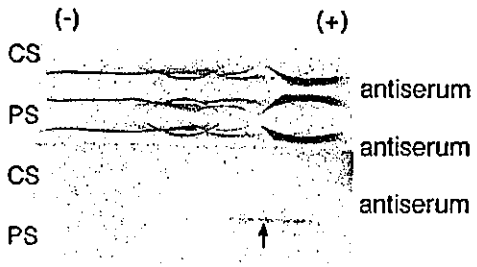

Figure 2 Immunoelectrophoresis and LD activity staining. After immunoelectrophoresis with rabbit antiserum against whole human serum, the precipitin lines were stained by Amido Black protein staining solution (upper half of the Figure) and LD activity visualizing solution (lower half). CS indicates control serum from a healthy volunteer and PS indicates the patient's serum. The arrow indicates an immunoprecipitin line possibly caused by a complex between LD and α_1-lipoprotein.

The patient did not have any cancers or hereditary variants. The extra LD isoenzyme electrophoretic band was caused by conjugation with α_1-lipoprotein. After absorption of α_1-lipoprotein with a specific antibody, the extra band disappeared. However, we do not understand why the precipitin line associated with anti-α_1-lipoprotein antiserum was not colored by LD activity staining and why the line associated with whole human serum antiserum was colored. All of the antisera or antibodies in this study were from immunized rabbits. The discrepancy might be due to a difference in methodologies. The complex between LD and α_1-lipoprotein might have dissociated upon mixing with α_1-lipoprotein antiserum. It was reported that a part of the LD-IgG complexes was dissociated by NAD, NADH or 5'-AMP (3, 5). Two possible consequences of dissociation are that the bound antiserum blocked LD binding or that α_1-lipoprotein changed conformationally upon reaction with the antiserum so that it could not conjugate with LD.

At the beginning of our study the extra band comprised 15% of the LD bands but after 7 months the percentage of the extra band decreased to 7% (data not shown). The high LD activity also decreased to within the reference interval. The extra band activity decreased with the decrease of the total LD activity. Because the proportion of the extra band did not seem to depend upon the disease activity, it might not be related to clinical symptoms or states. An extra electrophoretic band migrating between LD1 and LD2 is rare in a patient with mitral stenosis (14), and our patient with an identified conjugation with α_1-lipoprotein is, to our knowledge, the first reported. Therefore, the clinical significance of the extra band remains to be determined.

Acknowledgements

This research was supported in part by a Grant-in-Aid for Scientific Research (13470518) from the Ministry of Education, Science, Sports, Culture and Technology, Japan.

References

1. Maekawa M. Lactate dehydrogenase isoenzymes. J Chromatogr 1988;429:373–98.
2. Ganrot PO. Lupoid cirrhosis with serum lactic acid dehydrogenase linked to a gamma A immunoglobulin. Experientia 1967;23:593.
3. Gorus F, Aelbrecht W, Van Camp B. Circulating IgG-LD complex, dissociable by addition of NAD^+. Clin Chem 1982;28:236–9.

4. Sudo K, Maekawa M, Kanno T. Immunochemical properties of immunoglobulin G conjugated with lactate dehydrogenase. Clin Chem 1985;31:1178–81.
5. Fujita K, Sakurabayashi I, Kusanagi M, Kawai T. A lactate dehydrogenase-immunoglobulin G1 complex, not blocked by anti-idiotype antibody, in a patient with IgG1-lambda type M-proteinemia. Clin Chem 1987;33:1478–83.
6. Trocha PJ. Lactate dehydrogenase isoenzymes linked to beta-lipoproteins and immunoglobulin A. Clin Chem 1977;23:1780–3.
7. Kanno T, Sudo K, Kitamura M, Miwa S, Ichiyama A, Nishimura Y. Lactate dehydrogenase A-subunit and B-subunit deficiencies: comparison of the physiological roles of LDH isozymes. Isozymes, Curr Top Biol Med Res 1983;7:131–50.
8. Maekawa M, Sudo K, Kobayashi A, Sugiyama E, Li SSL, Kanno T. Fast-type electrophoretic variant of lactate dehydrogenase M(A) and comparison with other missense mutations in lactate dehydrogenase M(A) and H(B) genes. Clin Chem 1994;40:665–8.
9. Otsu N, Hirata M, Miyazawa K, Tuboi S. Abnormal lactate dehydrogenase isoenzyme in serum and tumor tissue of a patient with neuroblastoma. Clin Chem 1985;31:318–20.
10. Maekawa M, Inomata M, Sasaki MS, Kaneko A, Ushiama M, Sugano K, et al. Electrophoretic variant of lactate dehydrogenase isoenzyme and selective promoter methylation of the LDHA gene in a human retinoblastoma cell line. Clin Chem 2002;48:1938–45.
11. Baxi AJ, Bapat JP, Damle SR, Talavadekar RV, Rajpal RM, Dave JK. New laboratory method to detect hepatitis-B (Australia) antigen based on 'anomalous' lactate dehydrogenase isoenzyme. Vox Sang 1976;31:70–3.
12. Cabello B, Lubin J, Rywlin AM, Frenkel R. Significance of a sixth lactate dehydrogenase isoenzyme (LDH6). Am J Clin Pathol 1980;73:253–8.
13. Japanese Society of Clinical Chemistry. Recommended method for lactate dehydrogenase. Jpn J Clin Chem 1990;19:228–46.
14. Shibata H, Tozawa T, Morita Y, Taiko K. LDH anomaly by conjugation with serum protein component except immunoglobulins [abstract]. Jpn J Electroph 1983;27:262 (in Japanese).

CLINICAL GASTROENTEROLOGY AND HEPATOLOGY 2004;2:147–156

Extensive but Hemiallelic Methylation of the h*MLH1* Promoter Region in Early-Onset Sporadic Colon Cancers With Microsatellite Instability

YASUYUKI MIYAKURA,*,† KOKICHI SUGANO,*,§ TAKAYUKI AKASU,‖ TERUHIKO YOSHIDA,§ MASATO MAEKAWA,¶ SOH SAITOH,# HIDEYUKI SASAKI,** TADASHI NOMIZU,†† FUMIO KONISHI,†,§§ SHIN FUJITA,‖ YOSHIHIRO MORIYA,‖ and HIDEO NAGAI†

*Oncogene Research Unit/Cancer Prevention Unit, Tochigi Cancer Center Research Institute, Tochigi; †Department of Surgery, Jichi Medical School, Tochigi; §Genetic Counseling Clinic, National Cancer Center Hospital, Tokyo; ‖Department of Surgery, National Cancer Center Hospital, Tokyo; ¶Department of Laboratory Medicine, Hamamatsu Medical University, Hamamatsu; #Department of Gastroenterology, Aomori Prefectural Central Hospital, Aomori; **Department of Surgery, Hachinohe City Hospital, Aomori; ††Hoshi General Hospital, Fukushima; and §§Department of Surgery, Jichi Medical School, Omiya Medical Center, Saitama, Japan

Background & Aims: Methylation of the h*MLH1* promoter region is frequently observed in microsatellite instability (MSI)–positive sporadic colorectal carcinomas. We studied h*MLH1* promoter methylation in peripheral blood lymphocytes of 87 index patients representing 29 cases of hereditary nonpolyposis colorectal cancers (HNPCCs), 28 cases of atypical HNPCCs, and 30 sporadic cases of the development of early-onset colorectal carcinomas or multiple primary cancers. *Methods:* Methylation of the h*MLH1* promoter region was analyzed by Na-bisulfite polymerase chain reaction/single-strand conformation polymorphism analysis or methylation-specific polymerase chain reaction. MSI, allelic status of the h*MLH1* locus, and loss of hMLH1 protein expression were examined in cases for which tumor tissues were available. *Results:* Extensive methylation of the h*MLH1* promoter was detected in peripheral blood lymphocytes of 4 of 30 patients with sporadic early-onset colon cancer, among whom multiple primary cancers (1 colon and 1 endometrial cancer) developed in 2 cases. This methylation was not detected in analyses of HNPCC or atypical HNPCC groups or healthy control subjects. MSI was positive, and extensive methylation was detected in both cancers (colon and endometrial cancer) and normal tissues (colon, gastric mucosa, endometrium, and bone marrow) in all of the examined cases (3 of 3). Analysis of a polymorphic site in the h*MLH1* promoter in 2 informative cases showed that methylation was hemiallelic. In 1 case, the unmethylated allele was lost in the colon cancer but not in the metachronous endometrial cancer. *Conclusions:* Constitutive, hemiallelic methylation of the h*MLH1* promoter region was shown to be associated with carcinogenesis in sporadic, early-onset MSI-positive colon cancers.

Hereditary nonpolyposis colorectal cancer (HNPCC) is an autosomal dominantly inherited syndrome predisposing to cancers of the colorectum, endometrium, ovary, small intestine, and upper urinary tract.[1] The majority (85%–95%) of HNPCC tumors show microsatellite instability (MSI), which leads to the accumulation of deletion and insertion mutations at simple repeated sequences. In HNPCC, MSI is caused by germline mutations of mismatch repair genes (*MMR* genes) such as h*MSH2*, h*MLH1*, h*PMS1*, h*PMS2*, and h*MSH6*.[2–7] Among these *MMR* genes, mutations of h*MSH2* and h*MLH1* are known to be responsible for up to 45%–64% of HNPCCs.[8,9] HNPCCs are characterized phenotypically by early-onset colorectal carcinoma (CRC), prevalent tumor location in the proximal colon, and an increased risk of developing multiple CRCs and other malignancies.[10–13] On the other hand, some (10%–15%) sporadic CRCs also show MSI,[14–16] and methylation of the h*MLH1* promoter region has been suggested to be the major mechanism in these cases.[17–19] Methylation of the h*MLH1* promoter region and subsequent transcriptional silencing have been demonstrated in the formation of MSI-positive cancers.[17–21] In a previous study, methylation of the h*MLH1* promoter region induced transcriptional silencing of both of the h*MLH1* alleles in cell lines showing MSI[22] and this epigenetic mechanism of gene inactivation is in line with Knudson's two-hit hypothesis.[23] The proximal region of the h*MLH1* promoter contains cis-elements important for regulating gene expression.[24] Methylation of an adjacent CpG site inhibits binding of the core binding

Abbreviations used in this paper: BIPS, Na-bisulfite treatment and PCR single-strand conformation polymorphism; CRC, colorectal carcinoma; HNPCC, hereditary nonpolyposis colorectal cancer; LOH, loss of heterozygosity; *MMR* gene, mismatch repair gene; MSI, microsatellite instability; MSI-H, high-frequency MSI; MSP, methylation-specific PCR; PBL, peripheral blood lymphocyte; PCR, polymerase chain reaction; RT-PCR, reverse-transcription PCR; SSCP, single-strand conformation polymorphism.

1542-3565/04/$30.00
PII: 10.1053/S1542-3565(03)00314-8

factor to the CCAAT box in this region and is one of the causes of h*MLH1* gene silencing in colon cancer cells.[25] We reported that extensive methylation (designated as full methylation) of the h*MLH1* promoter region played a crucial role in h*MLH1* gene inactivation,[26] and that full methylation occurred in both alleles of the h*MLH1* promoter region in high-frequency MSI (MSI-H) colon cancers.[27] In one third of the CRCs showing full methylation, methylation was also detected in the adjacent normal colonic mucosa, although it was confined to the most upstream region of the h*MLH1* promoter sequences (designated as partial methylation).[27] Sporadic MSI-positive CRCs show different clinicopathological characteristics from those of HNPCC in that they are preferentially associated with late-onset proximal colon cancer in female patients,[26,28] suggesting that changes of hormonal status might be related to the development of the h*MLH1* promoter methylation. Recently, Gazzoli et al.[29] examined 14 cases of suspected HNPCC with MSI-H but no detectable germline mutations of h*MSH2*, h*MLH1*, and h*MSH6* for hypermethylation of the h*MLH1* promoter region, and they reported a case in which 1 allele of h*MLH1* was methylated in DNA isolated from blood, and biallelic inactivation of the h*MLH1* gene in the tumor was caused by a loss of heterozygosity (LOH) of the other allele. They suggested that this was a novel mode of germline inactivation of a cancer susceptibility gene.

In this study we analyzed the methylation status of the h*MLH1* promoter region in peripheral blood lymphocytes (PBLs) of patients referred to genetic counseling clinics because of the suspicion of an HNPCC. We detected constitutive methylation of the h*MLH1* promoter region in 4 cases of early-onset sporadic MSI-H CRCs. They displayed hemiallelic but full methylation of the h*MLH1* promoter region in normal tissues such as PBLs, normal colonic mucosa, endometrium, gastric mucosa, and bone marrow, exhibiting distinctly different clinical characteristics from both cases of HNPCC and cases of sporadic MSI-H CRC.

Materials and Methods

Patients

The study protocol was carried out after receiving institutional review board approval and written informed consent for the study from 87 index patients. PBLs were obtained from the 87 index patients, who visited genetic counseling clinics because of suspicion of HNPCC. All of these patients developed CRCs, and 29 of them fulfilled 1 of the 2 HNPCC criteria, i.e., the Amsterdam's minimum criteria or the modified Amsterdam criteria.[30–32] Twenty-eight kindred were classified as having atypical HNPCC, because they had at least 1 first-degree relative with CRC but did not fulfill the above-mentioned criteria. Of the kindred with atypical HNPCC, 13 kindred fulfilled the second (B-2) and/or fourth (B-4) criteria of the Bethesda guidelines,[33] i.e., individuals with 2 HNPCC-related cancers, including synchronous and metachronous CRCs or associated extracolonic cancers (5 cases) (B-2), individuals with CRC or endometrial cancer diagnosed at age younger than 45 years (6 cases) (B-4), and 2 cases fulfilled both of these 2 criteria (B-2 + B-4). Thirty kindred fulfilled neither the criteria for HNPCC nor atypical HNPCC. They developed early-onset CRCs when younger than the age of 50 years or multiple CRCs and/or extracolonic cancers, without showing familial predisposition to HNPCC-related tumors in their first-degree relatives. As to the relation with the Bethesda guidelines, the number of cases fulfilling the second or fourth criteria of the Bethesda guidelines was 4 (B-2), 20 (B-4), and 2 (B-2 + B-4), respectively. Regarding case H403, a case of sporadic CRC showing constitutive methylation of the h*MLH1* promoter region, the proband's sister visited the clinic for genetic counseling, and her PBLs were examined for methylation. The methylation status of the h*MLH1* promoter region was also examined in PBLs from 100 normal healthy control subjects older than 50 years undergoing routine health checkups. Before the analysis, samples were made unlinkable as to their personal information.

Analysis of MSI

In 4 cases showing aberrant methylation of the h*MLH1* promoter region, the MSI status was examined in all available samples, including tumor tissues and normal tissues such as PBLs, colonic mucosa, gastric mucosa, endometrium, and bone marrow aspirate. Genomic DNAs were subjected to polymerase chain reaction (PCR) amplification at 9 microsatellite repeat loci (*D2S123, D5S346, D17S250, BAT26, BAT25, MSH3, MSH6, TGFBR2,* and *BAX*). Analysis of MSI was performed as described previously.[26] The definition of MSI status was as follows: high-frequency MSI (MSI-H), when 30% or greater of the 9 markers showed MSI, in accordance with the recommendation of the National Cancer Institute Workshop.[34]

Methylation Analysis of the h*MLH1* Promoter Region

Na-bisulfite PCR/single-strand conformation polymorphism (SSCP) (BiPS) analysis was performed as described previously[26,35] (Figure 1). With the adenine residue at the start codon numbered as +1nt, the h*MLH1* promoter (−755 to +86) was divided into 5 regions (region A [from −755 to −574, containing 23 CpG sites], B [from −597 to −393, 12 CpG sites], C [from −420 to −188, 16 CpG sites], D [from −286 to −53, 13 CpG sites], and E [from −73 to +86, 13 CpG sites]) and was amplified with 5 sets of PCR primers. Each primer set was designed to anneal to both methylated and unmethylated DNAs, of which the amplicons could be separated by SSCP analysis. Amplified DNA fragments were visualized by using SYBR Gold nucleic acid gel stain (Cosmo Bio

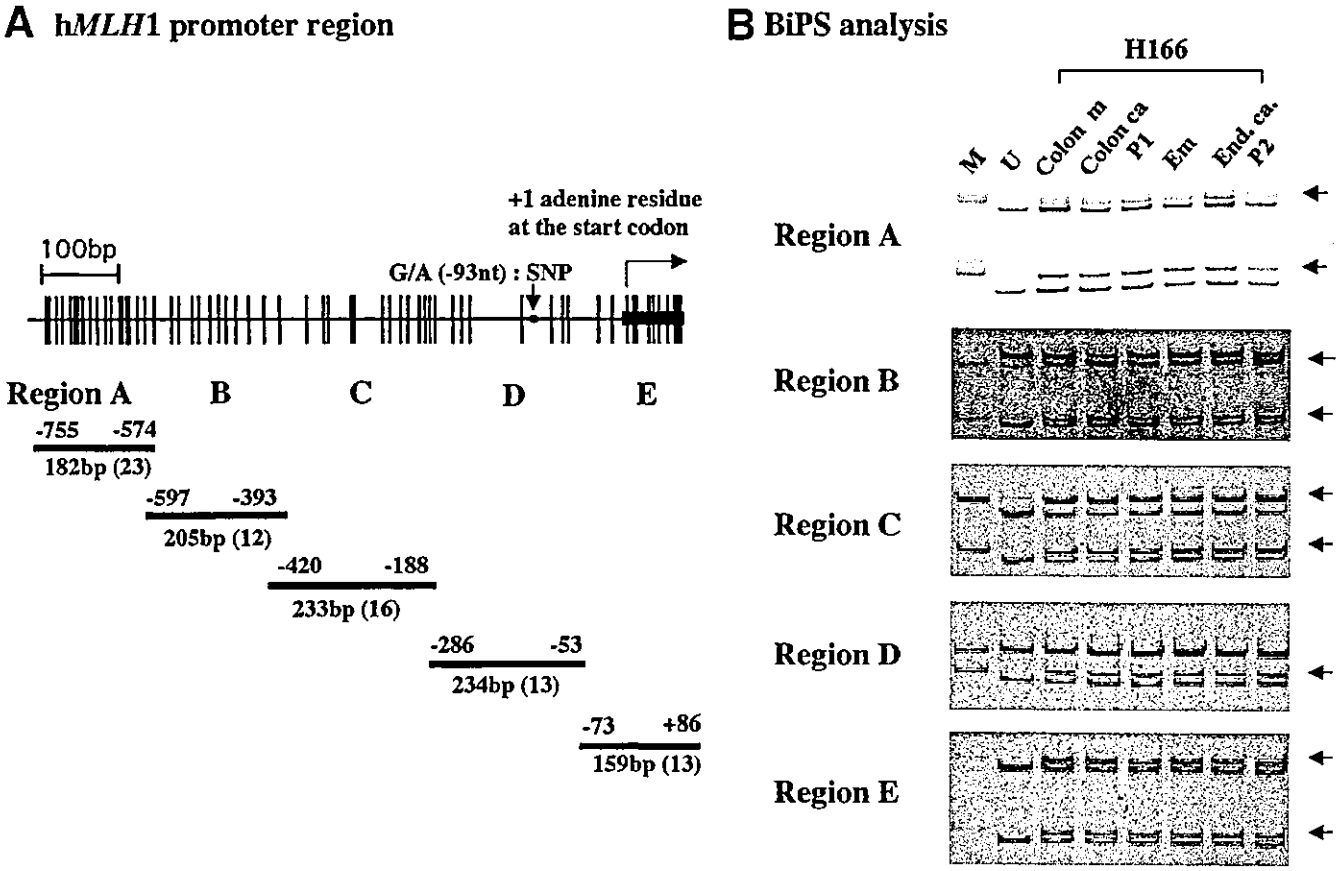

Figure 1. BiPS analysis of h*MLH1* promoter region and methylation profiles of various tissues in case H166. (*A*) Map of the 5′ CpG islands of the h*MLH1* gene. CpG sites are indicated by vertical lines. The arrow indicates G/A polymorphism at position −93nt in the h*MLH1* promoter region. The expected PCR products for regions A, B, C, D, and E are shown. Their positions relative to the adenine residue at the start codon and the sizes of the amplified DNA fragments are indicated. Figures in the parentheses indicate the numbers of CpG sites in each region. (*B*) Na-bisulfite treatment and PCR-SSCP (BiPS) analysis of the h*MLH1* promoter region in each tissue of case H166 (M, control methylated DNA; U, control unmethylated DNA; Colon m, colon normal mucosa; Colon ca, colon cancer; P1, PBLs obtained at 34 years of age (diagnosed with colon cancer); Em, endometrium; Eca, endometrial cancer; P2, PBLs obtained at 44 years of age (diagnosed with endometrial cancer). We divided the h*MLH1* promoter into 5 regions (regions A–E) and examined the methylation status. DNAs from all samples in case H166 showed methylated bands in all regions, indicating full methylation of the h*MLH1* promoter region, which was confirmed by direct sequencing of the mutated bands (data not shown).

Co., Tokyo, Japan) and scanned with a Fluorescent Image Analyzer Model FLA-3000G (Fuji Photo Film Co., Tokyo, Japan). When the bands showed mobility shifts, they were cut from the gel, reamplified, and directly sequenced without subcloning by using an ABI 310 PRISM sequencer (Perkin-Elmer Co., Branchburg, NJ) with a Big-Dye Terminator Cycle Sequencing Ready Reaction Kit (PE Applied Biosystems, Foster City, CA). Full methylation was defined as the state in which all CpG sites from regions A through E were methylated.[26,27] The allelic status of methylation was examined by direct sequencing of the G/A polymorphic site at −93nt in region D.[36] Furthermore, the methylation status of the h*MLH1* promoter region D was also analyzed by methylation-specific PCR (MSP) as described previously[27] (Figure 2*B* and *C*). The PCR product was mixed with 5× loading buffer, electrophoresed on a nondenaturing 8% polyacrylamide gel, stained with ethidium bromide, and scanned with a Fluorescent Image Analyzer Model FLA-3000G. DNA fragments amplified by MSP were subjected to direct sequencing, and G/A polymorphism was examined to determine whether the methylation was a biallelic or hemiallelic event.

Mutation Analysis of the h*MSH2* and h*MLH1* Genes

Total RNA was extracted from the PBLs treated with puromycin by using the acid guanidine phenol chloroform method.[37] Long reverse-transcription (RT)–PCR was carried out from RNAs extracted from PBLs incubated in the presence of puromycin, according to the method we reported previously.[38,39] Signals from mutated alleles are enhanced after puromycin treatment as a result of the suppression of nonsense-mediated mRNA decay and easily distinguishable from signals from the wild-type allele. This approach is a sensitive method to screen deleterious mutations such as nonsense or frameshift mutations and large genomic disorganizations resulting in genomic deletion or partial duplication of the h*MLH1* gene.[39] Sequencing reactions were performed by using a Big-Dye Terminator Cycle Sequencing Reaction kit. Elec-

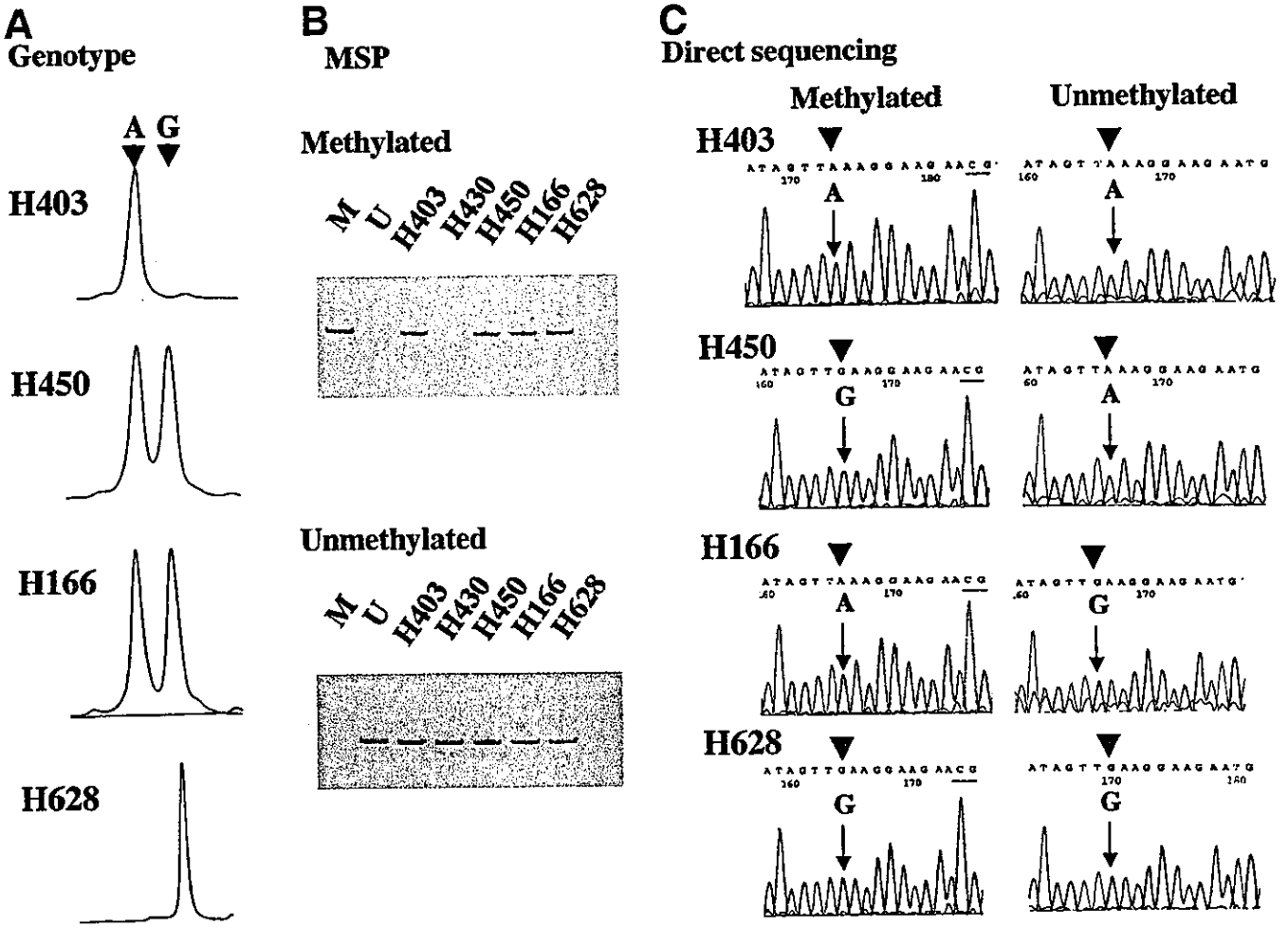

Figure 2. Uniparental methylation of the h*MLH1* promoter region. (*A*) PCR/SSCP analysis of the SNP at position −93nt was used to determine the genotype of 4 cases, i.e., A/A for H403, A/G for H450 and H166, and G/G for H628. (*B*) MSP analysis of the h*MLH1* promoter region D. M, control methylated DNA; U, control unmethylated normal DNA. DNA derived from H403, H450, H166, and H628 showed a methylated band in the promoter region D. DNA derived from H430 (unaffected sister of H403) did not show a methylated band. In addition, DNA derived from all cases showed an unmethylated band in the same region. (*C*) Direct sequencing of the PCR products derived from the methylated and unmethylated fragments in MSP analysis. The arrow indicates G/A polymorphism at position −93nt in the h*MLH1* promoter region. One allele (allele G in H450, allele A in H166) was observed to be a methylated fragment, and the other allele (allele A in H450, allele G in H166) was observed to be an unmethylated fragment.

trophoresis was carried out by using an ABI 310 PRISM sequencer. Primers used for direct sequencing were described in a previous report.[38] All mutations detected by direct sequencing were confirmed by PCR-based sequencing of the corresponding region of genomic DNA.

Analysis of Allelic Loss of h*MLH1*

Analysis of LOH of h*MLH1* was performed as described previously[27,40] (Figure 3). Briefly, an ALFexpress DNA sequencer (Pharmacia, Tokyo, Japan) was used for SSCP analysis. Electrophoresis was performed at 20W for 1500 minutes with a 15% polyacrylamide gel. During electrophoresis, the gel was kept at a constant temperature of 16°C by using a circulating water bath. The data were analyzed by using the software package Fragment Manager (Pharmacia, Tokyo, Japan). LOH was defined when the peak height of the signal from either allele was decreased more than 50% as compared with that of the normal control.

Immunohistochemical Examination of h*MLH1*

Immunohistochemistry was performed as described previously[26] (Figure 4). Briefly, tissue sections were deparaffinized with xylene and dehydrated by using a graded series of ethanol. Antigen retrieval was performed in citrate buffer by using a heat-induced microwave oven. The avidin-biotin–conjugated immunoperoxidase technique was performed by using a DAKO LSAB2 Kit (DAKO, Carpinteria, CA). Endogenous peroxidase activity was blocked by methanol supplemented with 0.02% H_2O_2. Sections were immersed in 4% commercial nonfat skim milk powder to inhibit nonspecific antibody binding. The sections were then incubated overnight

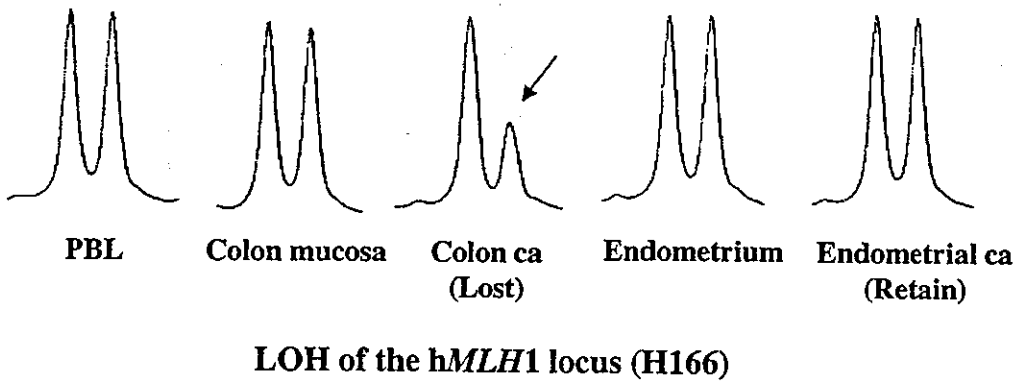

Figure 3. Electropherograms of SSCP analysis showing allelic loss of h*MLH1* in colon and endometrial tissues of case H166. Allelic loss was detected only in the colon cancer, and the position of the lost allele is indicated by an *arrow*.

with mouse monoclonal antibody to the h*MLH1* gene product (clone G168-15; PharMingen, San Diego, CA) (at a 1:50 dilution) and then with biotinylated secondary antibody and peroxidase-labeled avidin-biotin complex for 30 minutes, and staining was visualized by incubating the sections with 0.02% H_2O_2 and 0.02% diaminobenzidine in methanol for 10 minutes.

Results

Characteristics of Four Cases With Extensive Methylation of h*MLH1* Promoter Region in PBLs

Analysis of PBLs from 87 index patients in whom HNPCC was suspected revealed extensive methylation of the h*MLH1* promoter region in 4 cases (H166, H403, H450, and H628), whose characteristics are shown in Table 1. They were characterized by early-onset colon cancer and absence of family history of CRC in their first-degree relatives. Case H166 developed ascending colon cancer and endometrial cancer at the ages of 38 and 44 years, respectively, and PBL samples taken after the onset of each cancer showed extensive methylation of the h*MLH1* promoter region. Case H628 developed descending colon cancer at 29 years of age and had a history of left colectomy as a result of descending colon cancer at 17 years of age.

We examined MSI and methylation status of the h*MLH1* promoter region in colon cancer (H403, H166, and H628), endometrial cancer (H166) tissues, and in their normal counterparts (Figure 1*B*, Table 1). All of the

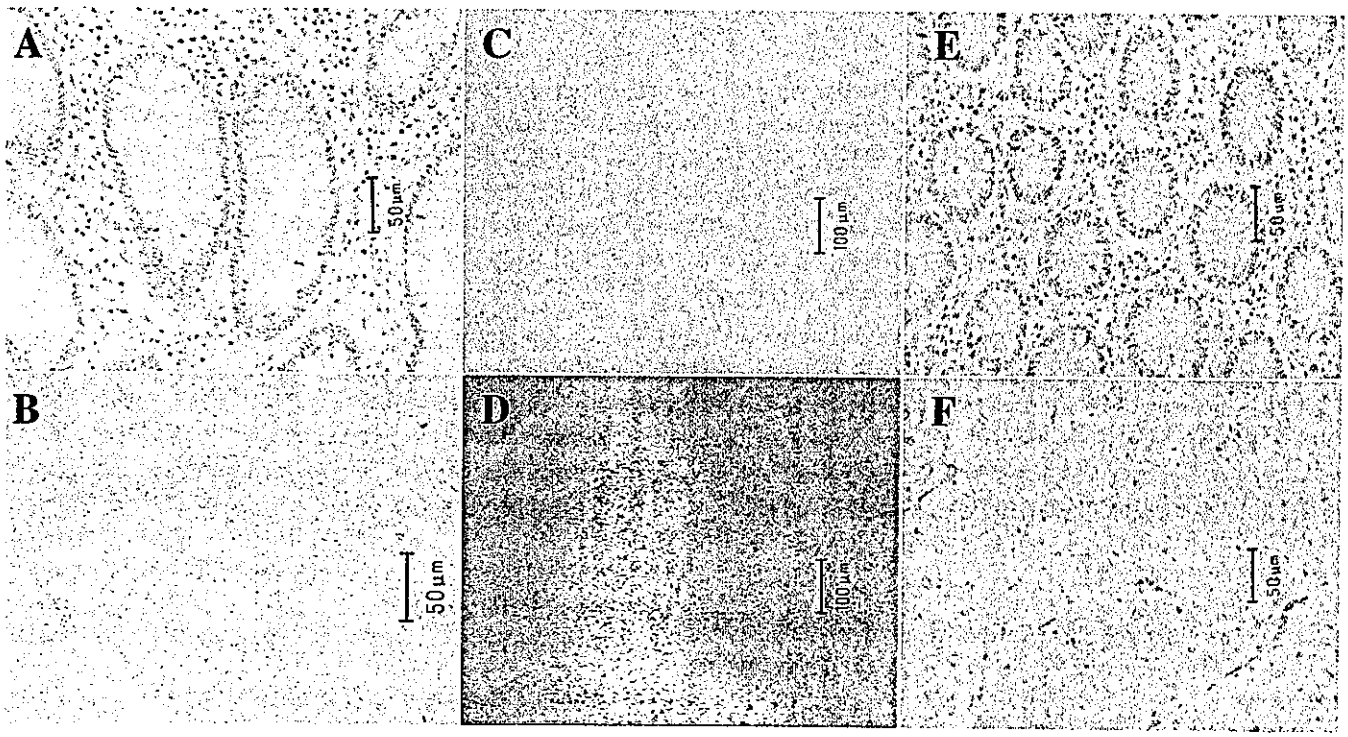

Figure 4. Immunohistochemical staining for h*MLH1* expression in colon tissues of case H166 (*A*, *B*) and H628 (*E*, *F*) and endometrial tissues of case H166 (*C*, *D*). Positive nuclear staining was observed in normal colonic mucosa (*A*, *E*) and endometrium (*C*), whereas a lack of positive nuclear staining was observed in carcinomas of the colon (*B*, *F*) and endometrium (*D*).

Table 1. Characteristics of Patients With Extensive Methylation of h*MLH1* Promoter Region in Lymphocyte Cells

Case	Age[a]	Sex	Site	Family history: CRC[b]	Family history: Other cancer	Genotype[c]	Specimen		MSI	h*MLH1*: Methylation	h*MLH1*: Mutation[d]	h*MLH1*: IHC	h*MSH2* mutation
H166	38	F	A	−	—	A/G	PBL	38 yr	MSS	Full	−		−
							Colon mucosa		MSS	Full		+	
							Colon cancer		MSI-H	Full		−	
							PBL	44 yr	MSS	Full	−		−
							Endometrium		MSS	Full		+	
							Endometrial cancer		MSI-H	Full		−	
							Colon mucosa	45 yr (biopsy)	MSS	Full			
							Gastric mucosa		MSS	Full			
							Bone marrow						
H403	28	M	T	−	Gastric cancer (grandfather)	A/A			MSS	Full	−		−
							PBL		MSS	Full		N.D.	
							Colon mucosa		MSI-H	Full		N.D.	
							Colon cancer						
H450	23	F	A	−	Pancreas cancer (grandmother)	A/G	PBL		MSS	Full	−		−
H628	29	M	D (17 yr)	−	Gastric cancer (grandfather)	G/G			MSS	Full	−		−
			A (29 yr)				PBL		MSS	N.D.		+	
					Breast cancer (aunt)		Colon mucosa		MSI-H	N.D.		−	
							Colon cancer	(biopsy)	MSS	Full			
					Breast cancer (aunt)		Colon mucosa	(biopsy)	MSS	Full			
							Gastric mucosa						

IHC, immunohistochemical analysis; A, ascending colon; MSS, MSI-stable; T, transverse colon; N.D., not done; D, descending colon; PBL, peripheral blood lymphocyte; MSI-H, high-frequency MSI; +, positive staining; −, negative staining.
[a]CRC onset age.
[b]No family history of CRC.
[c]h*MLH1* promoter genotype (−93 nt from translation start site).
[d]Mutation negative.

tumors showed MSI-H, and extensive methylation of the h*MLH1* promoter region was demonstrated in both tumors and normal mucosa. In cases H166 and H628, the patients underwent further examinations postoperatively such as digestive endoscopy (H166 and H628) and bone marrow aspiration (H166) for persistent leukopenia.

In both cases, methylation of the h*MLH1* promoter region was shown to be constitutive and hemiallelic in all samples examined. PBLs of case H403's sister (H430) did not show the methylation (Figure 2*B*). The PBLs of the other family members were not available. No germline mutations were detected in the h*MLH1* or h*MSH2* genes of these 4 patients. Methylation of the h*MLH1* promoter region was not detected in the PBLs of 100 healthy blood donors.

Hemiallelic Methylation of h*MLH1* Promoter Region in Normal Tissues

We previously reported that methylation of the h*MLH1* promoter region was a biallelic event in MSI-positive CRCs.[27] To determine whether methylation of the h*MLH1* promoter region in PBL is a biallelic epigenetic event, we examined the methylation status of this region by using G/A polymorphism at position −93nt in the h*MLH1* promoter by use of MSP combined with DNA sequencing (Figures 1 and 2*A*). In the 2 informative cases, we could confirm that methylation was hemiallelic (allele G in H450, allele A in H166) in all specimens.

Immunohistochemical Assessment of hMLH1 Protein Expression

To determine whether h*MLH1* gene inactivation was caused by extensive methylation of the h*MLH1* promoter region, we investigated hMLH1 protein expression in colon (cases H166 and H628) and endometrial (case H166) tissues by immunohistochemistry (Figure 4). hMLH1 protein expression was not detected in colon or endometrial cancer, but it was detected in normal colonic mucosa and endometrium.

Cause of Lack of hMLH1 Protein Expression in Cancer Tissues

To determine how the hemiallelic methylation of the h*MLH1* promoter region induced silencing of

hMLH1 protein expression in cancer tissues, we investigated the LOH of h*MLH1* in case H166 (Figure 3). Analysis of the colon cancer showed somatic loss of the G allele at the h*MLH1* locus, and biallelic inactivation of the h*MLH1* gene was caused by extensive methylation of allele A, followed by loss of the opposite allele. However, analysis of the endometrial cancer did not show LOH, and thus we could not identify the cause of the reduced expression of hMLH1 protein in endometrial cancer.

Discussion

In the present study we examined the methylation status of the h*MLH1* promoter region in 87 index patients in whom HNPCC was suspected. The 87 index cases included 30 cases that were sporadic but had developed early-onset CRCs or multiple primary cancers. We identified 4 of 30 sporadic cases with extensive methylation of the h*MLH1* promoter region in PBLs. They all developed CRCs at a very young age (the age at onset for a first cancer varied from 17 through 38 years of age), and there were no HNPCC-related cancers in their first-degree relatives. Analysis of 2 cases heterozygous for a G/A polymorphism at position −93nt showed that the methylation was hemiallelic (Figure 2*C*). These findings were in accord with those of a case reported by Gazzoli et al.[29] Those authors reported hypermethylation of the h*MLH1* promoter region in 1 allele in the DNA from PBLs of a CRC patient with young age (25 years) at onset and without family history of CRC. We examined the methylation status of the h*MLH1* promoter region in DNAs from various tissues, including normal mucosa of the colon, stomach, and endometrium and bone marrow, and the methylation was invariably detected in all tissues examined. Methylation occurred as a constitutive, hemiallelic event. All of these 4 cases were early-onset, and they were also sporadic without family history of HNPCC-related tumors in their first-degree relatives. PBLs of case H403's sister (H430) did not show the methylation (Figure 2*B*). The PBLs of the other family members were not available. Constitutive methylation of the h*MLH1* promoter region was not detected in analyses of HNPCC or atypical HNPCC groups or healthy control subjects. Taken together, these findings suggest that hemiallelic methylation was not heritable, and that it was inconsistent with the mode of autosomal dominant mendelian inheritance, although aberrant methylation might be due to other unknown genetic mechanisms.

In MSI-H CRCs, methylation of the h*MLH1* promoter region has been reported to be extensive, usually occurring in both alleles of the h*MLH1* promoter, and strong association has been observed between the methylation profile of the h*MLH1* promoter region and the clinicopathologic background of the cases, i.e., preferential occurrence in the proximal colon, female predominance, and older age at onset.[26,28] The 4 cases studied here showed different characteristics from ordinary MSI-H tumors in that the methylation was a constitutive but hemiallelic event, preferentially observed in early-onset CRC and without gender specificity (2 male and 2 female patients). The frequency of constitutive methylation of the h*MLH1* promoter region was 13.3% (4 of 30 cases) in the cases of sporadic CRCs we examined, suggesting that hemiallelic methylation of the h*MLH1* promoter region accounts for a subset of early-onset sporadic CRCs with MSI-H. Liu et al.[41] identified 1 case of germline mutation in early-onset CRC showing MSI, but the previously reported rates of detection of mutations in the *MMR* genes in early-onset CRCs were low.[42–44] A study of 31 patients younger than 35 years of age and not fulfilling the Amsterdam minimum criteria, in which MSI was exhibited in 18 cases (58%), was also reported.[45] Twelve of those cases were evaluated for alterations of *MMR* genes, and 5 (42%) were found to harbor germline mutations of either h*MSH2* or h*MLH1*. Germline mutations of *MMR* genes might account for a part of early-onset CRCs, and some of them are suspected to be de novo mutations.

In our analysis of 30 sporadic cases, we detected 3 cases of germline mutations of the *MMR* genes (data not shown), whereas no germline mutations of h*MSH2* or h*MLH1* were detected in analyses of the 4 patients described here. Genomic disorganizations such as large deletions or duplications of the *MMR* genes have been thought to occur in a considerable proportion of HNPCC cases.[46,47] Previously, we reported 2 cases of genomic deletion and 1 case of partial duplication of the h*MLH1* gene that were detected by using long RT-PCR from puromycin-treated samples, and this method is sensitive enough to screen large genomic disorganizations of the *MMR* genes.[39] Recently, several genes were reported to be involved in familial predisposition to CRC.[48–50] In the case of h*MSH6*, many of the mutation carriers develop carcinomas of the distal colon and endometrium, and analysis of tumor tissues showed that half of them were MSI-negative.[48] As for MYH, the mutation carriers showed autosomal recessive inheritance, whereas their phenotypes were characterized by the presence of multiple colorectal adenomas.[49,50] The clinical characteristics of our cases seem to be incompatible with mutations of these 2 genes.

In case H166, biallelic inactivation of the h*MLH1* gene in colon cancer was caused by an LOH of the

unmethylated allele (Figure 3). Gazzoli et al.[29] reported that biallelic inactivation resulted in loss of hMLH1 protein expression in the tumor and suggested a novel mode of germline inactivation of a cancer susceptibility gene. These results were inconsistent with our previous study showing that allelic loss of the h*MLH1* locus was infrequent, and methylation was biallelic in the majority of the ordinary MSI-H sporadic CRCs.[27] All of the 4 cases examined here were postoperative, and it remains unclear when the methylation of the h*MLH* gene occurred.

In case H166, the patient developed ascending colon cancer at the age of 38 years and endometrial cancer at the age of 44 years. In case H628, the patient developed descending colon cancer at the age of 17 years and ascending colon cancer at the age of 29 years (Table 1). In retrospective analysis, MSI-positive sporadic CRC patients have been reported to be at risk for developing extracolonic cancers and metachronous multiple CRCs.[51–54] Full methylation of the h*MLH1* promoter region in PBLs might have a significant influence on the carcinogenesis of these multiple primary cancers and might be a potent diagnostic marker for identifying individuals at high risk of developing cancer.

In conclusion, we have tentatively identified a rare group of patients who have the MSI-H phenotype, show early-onset colon cancers without a family history of CRC, and exhibit extensive but hemiallelic methylation of the h*MLH1* promoter region in PBLs and other normal tissues.

References

1. Lynch HT, de la Chapelle A. Genetic susceptibility to non-polyposis colorectal cancer. J Med Genet 1999;36:801–818.
2. Fishel R, Lescoe MK, Rao MR, Copeland NG, Jenkins NA, Garber J, Kane M, Kolodner R. The human mutator gene homolog MSH2 and its association with hereditary nonpolyposis colon cancer. Cell 1993;75:1027–1038.
3. Leach FS, Nicolaides NC, Papadopoulos N, Liu B, Jen J, Parsons R, Peltomaki P, Sistonen P, Aaltonen LA, Nystrom-Lahti M, Guan XY, Zhang J, Meltzer PS, Yu JW, Kao FT, Chen DJ, Carosaletti KM, Fournier REK, Todd S, Lewis T, Leach RJ, Naylor SL, Weissenbach J, Mecklin JP, Jarvinen H, Petersen GM, Hamilton SR, Green J, Jass J, Watson P, Lynch HT, Trent JM, de la Chapelle A, Kinzler KW, Vogelstein B. Mutations of a mutS homolog in hereditary nonpolyposis colorectal cancer. Cell 1993;75:1215–1225.
4. Bronner CE, Baker SM, Morrison PT, Warren G, Smith LG, Lescoe M, Kane M, Earabino C, Lipford J, Lindblom A, Tannergard P, Bollag RJ, Godwin AR, Ward DC, Nordenskjold M, Fishel R, Kolodner R, Liskay RM. Mutation in the DNA mismatch repair gene homologue hMLH1 is associated with hereditary non-polyposis colon cancer. Nature 1994;368:258–261.
5. Nicolaides NC, Papadopoulos N, Liu B, Wei YF, Carter KC, Ruben SM, Rosen CA, Haseltine WA, Fleischmann RD, Fraser CM, Adams MD, Venter JC, Dunlop MG, Hamilton SR, Petersen GM, de la Chapelle A, Vogelstein B, Kinzler KW. Mutations of two PMS homologues in hereditary nonpolyposis colon cancer. Nature 1994;371:75–80.
6. Papadopoulos N, Nicolaides NC, Wei YF, Ruben SM, Carter KC, Rosen CA, Haseltine WA, Fleischmann RD, Fraser CM, Adams MD, Venter JC, Hamilton SR, Petersen GM, Watson P, Lynch HT, Peltomaki P, Mecklin JP, de la Chapelle A, Kinzler KW, Vogelstein B. Mutation of a mutL homolog in hereditary colon cancer. Science 1994;263:1625–1629.
7. Akiyama Y, Sato H, Yamada T, Nagasaki H, Tsuchiya A, Abe R, Yuasa Y. Germ-line mutation of the hMSH6/GTBP gene in an atypical hereditary nonpolyposis colorectal cancer kindred. Cancer Res 1997;57:3920–3923.
8. Liu B, Parsons R, Papadopoulos N, Nicolaides NC, Lynch HT, Watson P, Jass JR, Dunlop M, Wyllie A, Peltomaki P, de la Chapelle A, Hamilton SR, Vogelstein B, Kinzler KW. Analysis of mismatch repair genes in hereditary non-polyposis colorectal cancer patients. Nat Med 1996;2:169–174.
9. Wijnen J, Khan PM, Vasen H, van der Klift H, Mulder A, van Leeuwen-Cornelisse I, Bakker B, Losekoot M, Moller P, Fodde R. Hereditary nonpolyposis colorectal cancer families not complying with the Amsterdam criteria show extremely low frequency of mismatch-repair-gene mutations. Am J Hum Genet 1997;61:329–335.
10. Mecklin JP, Jarvinen HJ. Tumor spectrum in cancer family syndrome (hereditary nonpolyposis colorectal cancer). Cancer 1991; 68:1109–1112.
11. Lynch HT, Smyrk TC, Watson P, Lanspa SJ, Lynch JF, Lynch PM, Cavalieri RJ, Boland CR. Genetics natural history, tumor spectrum, and pathology of hereditary nonpolyposis colorectal cancer: an updated review. Gastroenterology 1993;104:1535–1549.
12. Aarnio M, Mecklin JP, Aaltonen LA, Nystrom-Lahti M, Jarvinen HJ. Life-time risk of different cancers in hereditary non-polyposis colorectal cancer (HNPCC) syndrome. Int J Cancer 1995;64: 430–433.
13. Kinzler KW, Vogelstein B. Lessons from hereditary colorectal cancer. Cell 1996;87:159–170.
14. Aaltonen LA, Peltomaki P, Leach FS, Sistonen P, Pylkkanen L, Mecklin JP, Javinen H, Powell SM, Jen J, Hamilton SR, Petersen GM, Kinzler KW, Vogelstein B, Chapelle A. Clues to the pathogenesis of familial colorectal cancer. Science 1993;260:812–816.
15. Thibodeau SN, Bren G, Schaid D. Microsatellite instability in cancer of the proximal colon. Science 1993;260:816–819.
16. Kim H, Jen J, Vogelstein B, Hamilton SR. Clinical and pathological characteristics of sporadic colorectal carcinomas with DNA replication errors in microsatellite sequences. Am J Pathol 1994; 145:148–156.
17. Kane MF, Loda M, Gaida GM, Lipman J, Mishra R, Goldman H, Jessup JM, Kolodner R. Methylation of the hMLH1 promoter correlates with lack of expression of hMLH1 in sporadic colon tumors and mismatch repair-defective human tumor cell lines. Cancer Res 1997;57:808–811.
18. Cunningham JM, Christensen ER, Tester DJ, Kim CY, Roche PC, Burgart LJ, Thibodeau SN. Hypermethylation of hMLH1 promoter in colon cancer with microsatellite instability. Cancer Res 1998; 58:3455–3460.
19. Herman JG, Umar A, Polyak K, Graff JR, Ahuja N, Issa JP, Markowitz S, Willson JK, Hamilton SR, Kinzler KW, Kane MF, Kolodner RD, Vogelstein B, Kunkel TA, Baylin SB. Incidence and functional consequences of hMLH1 promoter hypermethylation in colorectal carcinoma. Proc Natl Acad Sci U S A 1998;95:6870–6875.
20. Esteller M, Levine R, Baylin SB, Ellenson LH, Herman JG. MLH1 promoter hypermethylation is associated with the microsatellite instability phenotype in sporadic endometrial carcinomas. Oncogene 1998;17:2413–2417.
21. Leung SY, Yuen ST, Chung LP, Chu KM, Chan AS, Ho JC. hMLH1 promoter methylation and lack of hMLH1 expression in sporadic

gastric carcinomas with high-frequency microsatellite instability. Cancer Res 1999;59:159–164.
22. Veigl ML, Kasturi L, Olechnowicz J, Ma A, Lutterbaugh JD, Periyasamy S, Li G-M, Drummond J, Modrich PL, Sedwick WD, Markowitz SD. Biallelic inactivation of h*MLH1* by epigenetic gene silencing, a novel mechanism causing human MSI cancers. Proc Natl Acad Sci U S A 1998;95:8698–8702.
23. Jones PA, Laird PW. Cancer epigenetics comes of age. Nat Genet 1999;21:163–167.
24. Deng G, Chen A, Hong J, Chae HS, Kim YS. Methylation of CpG in a small region of the hMLH1 promoter invariably correlates with the absence of gene expression. Cancer Res 1999;59:2029–2033.
25. Deng G, Chen A, Pong E, Kim YS. Methylation in hMLH1 promoter interferes with its binding to transcription factor CBF and inhibits gene expression. Oncogene 2001;20:7120–7127.
26. Miyakura Y, Sugano K, Konishi F, Ichikawa A, Maekawa M, Shitoh K, Igarashi S, Kotake K, Koyama Y, Nagai H. Extensive methylation of h*MLH1* promoter region predominates in proximal colon cancer with microsatellite instability. Gastroenterology 2001;121:1300–1309.
27. Miyakura Y, Sugano K, Konishi F, Fukayama N, Igarashi S, Kotake K, Matsui T, Koyama Y, Maekawa M, Nagai H. Methylation profile of the MLH1 promoter region and their relationship to colorectal carcinogenesis. Genes Chromosomes Cancer 2003;36:17–25.
28. Young J, Simms LA, Biden KG, Wynter C, Whitehall V, Karamatic R, George J, Goldblatt J, Walpole I, Robin SA, Borten MM, Stitz R, Searle J, McKeone D, Fraser L, Purdie DR, Podger K, Price R, Buttenshaw R, Walsh MD, Barker M, Leggett BA, Jass JR. Features of colorectal cancers with high-level microsatellite instability occurring in familial and sporadic settings: parallel pathways of tumorigenesis. Am J Pathol 2001;159:2107–2116.
29. Gazzoli I, Loda M, Garber J, Syngal S, Kolodner RD. A hereditary nonpolyposis colorectal carcinoma case associated with hypermethylation of the MLH1 gene in normal tissue and loss of heterozygosity of the unmethylated allele in the resulting microsatellite instability-high tumor. Cancer Res 2002;62:3925–3928.
30. Benatti P, Sassatelli R, Roncucci L, Pedroni M, Fante R, Di Gregorio C, Losi L, Gelmini R, Ponz de Leon M. Tumour spectrum in hereditary non-polyposis colorectal cancer (HNPCC) and in families with "suspected HNPCC": a population-based study in northern Italy—Colorectal Cancer Study Group. Int J Cancer 1993;54:371–377.
31. Bellacosa A, Genuardi M, Anti M, Viel A, Ponz de Leon M. Hereditary nonpolyposis colorectal cancer: review of clinical, molecular genetics, and counseling aspects. Am J Med Genet 1996;62:353–364.
32. Syngal S, Fox EA, Li C, Dovidio M, Eng C, Kolodner RD, Garber JE. Interpretation of genetic test results for hereditary nonpolyposis colorectal cancer. JAMA 1999;282:247–253.
33. Rodriguez-Bigas MA, Boland CR, Hamilton SR, Henson DE, Jass JR, Khan PM, Lynch H, Perucho M, Smyrk T, Sobin L, Srivastava S. A National Cancer Institute workshop on hereditary nonpolyposis colorectal cancer syndrome: meeting highlights and Bethesda guidelines. J Natl Cancer Inst 1997;89:1758–1762.
34. Boland CR, Thibodeau SN, Hamilton SR, Sidransky D, Eshleman JR, Burt RW, Meltzer SJ, Rodriguez-Bigas MA, Fodde R, Ranzani GN, Srivastava S. A National Cancer Institute workshop on microsatellite instability for cancer detection and familial predisposition: development of international criteria for the determination of microsatellite instability in colorectal cancer. Cancer Res 1998;58:5248–5257.
35. Maekawa M, Sugano K, Kashiwabara H, Ushiama M, Fujita S, Yoshimori M, Kakizoe T. DNA methylation analysis using bisulfite treatment and PCR-single-strand conformation polymorphism in colorectal cancer showing microsatellite instability. Biochem Biophys Res Commun 1999;262:671–676.
36. Ito E, Yanagisawa Y, Iwahashi Y, Suzuki Y, Nagasaki H, Akiyama Y, Sugano S, Yuasa Y, Maruyama K. A core promoter and a frequent single-nucleotide polymorphism of the mismatch repair gene hMLH1. Biochem Biophys Res Commun 1999;256:488–494.
37. Chomczynski P, Sacchi N. Single-step method of RNA isolation by acid guanidinium thiocyanate-phenol-chloroform extraction. Anal Biochem 1987;162:156–159.
38. Nomura S, Sugano K, Kashiwabara H, Taniguchi T, Fukayama N, Fujita S, Akasu T, Moriya Y, Ohhigashi S, Kakizoe T, Sekiya T. Enhanced detection of deleterious and other germline mutations of hMSH2 and hMLH1 in Japanese hereditary nonpolyposis colorectal cancer kindreds. Biochem Biophys Res Commun 2000;271:120–129.
39. Sumitsuji I, Sugano K, Matsui T, Fukayama N, Yamaguchi K, Akasu T, Fujita S, Moriya Y, Yokoyama R, Nomura S, Yoshida T, Kodama T, Ogawa M. Frequent genomic disorganisation of MLH1 in hereditary non-polyposis colorectal cancer (HNPCC) screened by RT-PCR on puromycin treated samples. J Med Genet 2003;40:e30.
40. Sugano K, Nakashima Y, Yamaguchi K, Fukayama N, Maekawa M, Ohkura H, Kakizoe T, Sekiya T. Sensitive detection of loss of heterozygosity in the TP53 gene in pancreatic adenocarcinoma by fluorescence-based single-strand conformation polymorphism analysis using blunt-end DNA fragment. Genes Chromosomes Cancer 1996;15:157–164.
41. Liu B, Nicolaides NC, Markowitz S, Willson LKV, Parsons R, Jen J, Papadopoulos N, Peltomaki P, de la Chapelle A, Hamilton SR, Kinzler KW, Vogelstein B. Mismatch repair gene defects in sporadic colorectal cancers with microsatellite instability. Nat Genet 1995;2:48–55.
42. Yuan Y, Han HJ, Zheng S, Park JG. Germline mutations of hMLH1 and hMSH2 genes in patients with suspected hereditary nonpolyposis colorectal cancer and sporadic early-onset colorectal cancer. Dis Colon Rectum 1998;41:434–440.
43. Verma L, Kane MF, Brassett C, Schmeits J, Evans DG, Kolodner RD, Maher ER. Mononucleotide microsatellite instability and germline MSH6 mutation analysis in early onset colorectal cancer. J Med Genet 1999;36:678–682.
44. Shin KH, Shin JH, Kim JH, Park JG. Mutational analysis of promoters of mismatch repair genes hMSH2 and hMLH1 in hereditary nonpolyposis colorectal cancer and early onset colorectal cancer patients: identification of three novel germ-line mutations in promoter of the hMSH2 gene. Cancer Res 2002;62:38–42.
45. Liu B, Farrington SM, Petersen GM, Hamilton SR, Parsons R, Papadopoulos N, Fujiwara T, Jen J, Kinzler KW, Wyllie A, Vogelstein B, Dunlop M. Genetic instability occurs in the majority of young patients with colorectal cancer. Nat Med 1995;1:348–352.
46. Wijnen J, van der Klift H, Vasen H, Khan PM, Menko F, Tops C, Meijers Heijboer H, Lindhout D, Moller P, Fodde R. MSH2 genomic deletions are a frequent cause of HNPCC. Nat Genet 1998;20:326–328.
47. Gille JJ, Hogervorst FB, Pals G, Wijnen JT, van Schooten RJ, Dommering CJ, Meijer GA, Craanen ME, Nederlof PM, de Jong D, McElgunn CJ, Schouten JP, Menko FH. Genomic deletions of MSH2 and MLH1 in colorectal cancer families detected by a novel mutation detection approach. Br J Cancer 2002;87:892–897.
48. Berends MJ, Wu Y, Sijmons RH, Mensink RG, van der Sluis T, Hordijk-Hos JM, de Vries EG, Hollema H, Karrenbeld A, Buys CH, van der Zee AG, Hofstra RM, Kleibeuker JH. Molecular and clinical characteristics of MSH6 variants: an analysis of 25 index carriers of a germline variant. Am J Hum Genet 2002;70:26–37.
49. Jones S, Emmerson P, Maynard J, Best JM, Jordan S, Williams GT, Sampson JR, Cheadle JP. Biallelic germline mutations in MYH predispose to multiple colorectal adenoma and somatic G:C→T:A mutations. Hum Mol Genet 2002;11:2961–2967.

50. Al-Tassan N, Chmiel NH, Maynard J, Fleming N, Livingston AL, Williams GT, Hodges AK, Davies DR, David SS, Sampson JR, Cheadle JP. Inherited variants of MYH associated with somatic G:C→T:A mutations in colorectal tumors. Nat Genet 2002;30:227–232.
51. Horii A, Han HJ, Shimada M, Yanagisawa A, Kato Y, Ohta H, Yasui W, Tahara E, Nakamura Y. Frequent replication errors at microsatellite loci in tumors of patients with multiple primary cancers. Cancer Res 1994;54:3373–3375.
52. Masubuti S, Konishi F, Togashi K, Okamoto T, Senba S, Shitoh K, Kashiwagi H, Kanazawa K, Tsukamoto T. The significance of microsatellite instability in predicting the development of metachronous multiple colorectal carcinomas in patients with nonfamilial colorectal carcinoma. Cancer 1999;85:1917–1924.
53. Yamashita K, Arimura Y, Kurosawa S, Itoh F, Endo T, Hirata K, Imamura A, Kondo M, Sato T, Imai K. Microsatellite instability in patients with multiple primary cancers of the gastrointestinal tract. Gut 2000;46:790–794.
54. Shitoh K, Konishi F, Miyakura Y, Togashi K, Okamoto T, Nagai H. Microsatellite instability as a marker in predicting metachronous multiple colorectal carcinomas after surgery: a cohort-like study. Dis Colon Rectum 2002;45:329–333.

Address reprint requests to: Kokichi Sugano, M.D., Oncogene Research Unit/Cancer Prevention Unit, Tochigi Cancer Center Research Institute, 4-9-13 Yohnan, Utsunomiya, Tochigi 320-0834, Japan. e-mail: ksugano@tcc.pref.tochigi.jp; fax: (81) 28-684-5756.

Supported in part by Grants-in-Aid for Cancer Research and for the Second Term Comprehensive 10-Year Strategy for Cancer Control from the Ministry of Health, Labor and Welfare, Japan, and a Grant-in-Aid from Public Trust Haraguchi Memorial Cancer Research Fund.

The authors thank Ayumi Kobayashi, Eri Yamauchi, and Noriko Fukayama for their excellent technical assistance and Nanri Fujiwara for her secretarial work.

complication, despite the repeat MRI showing a small residual tumour.

REFERENCES

1. Ariel L, Barkan MD, Wiliam F, Chandler MD. Giant pituitary prolactinoma with falsely low serum prolactin: the pitfall of the " High-dose Hook Effect": Case report. Neurosurgery 1998; 42: 913–916.
2. Bannister P, Sheridan P. Continued growth of a large pituitary prolactinoma despite high dose bromocriptine. Br J Clin Pract 1987; 41: 712–713.
3. Bloom H. Radiotherapy of pituitary tumours. In: Jenkins JS (ed) Pituitary Tumours. Butterworth, London 1973; 165–197.
4. Brediahl HD, Topliss DJ, Pike JW. Failure of bromocriptine to maintain reduction in size of a macroprolactinoma. Br Med J 1983; 287: 451–452.
5. Ciric I, Mikhael M, Stafford T, Lawson L, Garces R. Transsphenoidal microsurgery of pituitary macroadenomas with long-term follow-up results. J Neurosurg 1983; 59: 395–401.
6. Cohen R, Cooper P, Kupersmith M, Flamm E, Ransohoff J. Visual outcome after transsphenoidal removal of pituitary adenomas. Neurosurgery 1985; 17: 446–452.
7. Cohen DL, Diengdoh JV, Thomas DGT, Himsworth RL. An intracranial metastasis from a prolactin secreting pituitary tumour. Clin Endocrinol 1983; 18: 259–264.
8. Flickinger J, Nelson P, Taylor F. Incidence of cerebral infarction after radiotherapy for pituitary adenoma. Cancer 1989; 63: 2504–2508.
9. Fisher BJ, Gaspar LE, Noone B. Giant pituitary adenomas: role of radiotherapy. Int J Radiat Oncol Biol Phys 1993; 25: 677–681.
10. Gasser RW, Fikenstedt G, Skrabal F et al. Multiple intracranial metastases from a prolactin secreting pituitary tumour. Clin Endocrinol 1985; 22: 17–27.
11. Goel A, Nadkarni T. Surgical management of giant pituitary tumours: a review of 30 cases. Acta Neurochir (Wien) 1996; 138: 1042–1049.
12. Grebe SK, Delahunt JW, Feek CM. Treatment of extensively invasive (giant) prolactinomas with bromocriptine. NZ Med J 1992; 105: 129–131.
13. Grossman A, Besser GM. Prolactinomas. Br Med J 1985; 290: 182–184.
14. Laws Jr J, Trautmann J, Hollenburst J. Transsphenoidal decompression of the optic nerve and chiasm-visual results in 62 patients. J Neurosurg 1977; 46: 717–722.
15. Martin NA, Hales M, Wilson CB. Cerebellar metastasis from a prolactinoma during treatment with bromocriptine. J Neurosurg 1981; 55: 615–619.
16. Miyai K, Ichihara K, Kondo K, Mori S. Asymptomatic hyperprolactinemia and prolactinoma in the general population – mass screening by paired assays of serum prolactin. Clin Endocrinol (Oxf) 1986; 25: 549.
17. Mohr G, Hardy J, Comtois R, Beau-regard H. Surgical management of giant pituitary adenomas. Can J Neurol Sci 1990; 17: 62–66.
18. Molitch ME, Elton RL, Blackwell RE et al. Bromocriptine as primary therapy for prolactin-secreting macroadenomas: results of a multicenter study. J Clin Endocrinol Metab 1985; 60: 698–705.
19. Muphy FY, Vesely DL, Jordan RM, Flanigan S, Kohler PO. Giant invasive prolactinomas. Am J Med 1987; 83: 995–1002.
20. Nabarro JDN. Pituitary prolactinomas. Clin Endocrinal 1982; 17: 129–155.
21. Perani D, Colombo N, Scotti G, Tondon C. Rapid size reduction of giant prolactinoma following medical treatment. J Comp Assist Tomogr 1984; 8: 131–133.
22. Randall R, Laws E, Abboud C, Ebersold M, Kao P, Schiethauer B. Transsphenoidal microsurgical treatment of prolactin-producing pituitary adenomas. Mayo Clin Proc 1983; 58: 108–121.
23. Scherrer H, Turpin G, De Gennes JL, Schaison Cusin M, Heshmati HM, Thibierge M, Metzger J. Resultats du traitement par Bromocriptine des adenomas prolactine geants ou expansifs: A propos de 20 observations. Ann Med Interne (Paris) 1985; 136: 459–466.
24. Serri O, Rosio E, Beauregard H, Hardy J, Somma M. Recurrence of hyperprolactinemia after transsphenoidal adenomectomy in women with prolactinoma. N Eng J Med 1983; 309: 280–283.
25. Stefanis G, Cavanaugh H, Tindall G. Ophthalmological aspects of pituitary tumours. In: Tindall GJ, Collins WF (eds) Clinical Managements of Pituitary Disorders. Raven Press, New York 1979; 230–263.
26. Thorner MO, Perryman RL, Rogol AD et al. Rapid changes in prolactinoma volume after withdrawal and reinstitution of bromocriptine. J Clin Endocrinol Metab 1981; 53: 480–483.
27. Thorner MO, Schram HF, Evans WS, Rogol AD, Morris J, MacLeod RM. A broad spectrum of prolactin suppression by bromocriptine level after acute and chronic administration of bromocriptine. J Clin Endocrinol Metab 1980; 50: 1026–1033.
28. UHS, Johnso C. Metastatic prolactin-secreting pituitary adenoma. Hum Pathol 1984;15:94-96.
29. Iwai Y, Hakuba A, Khosla VK, Ch M, Nishikawa M, Katsuyama J, Inoue Y. Giant basal prolactinoma extending into the nasal cavity. Surg Neurol 1992; 37: 280–283.

Gross total surgical removal of malignant glioma from the medulla oblongata: report of two adult cases with reference to surgical anatomy

Kazuhiko Kyoshima[1] MD, Keiichi Sakai[1] MD, Tetsuya Goto[1] MD, Akihiko Tanabe[1] MD, Atsushi Sato[1] MD, Hisashi Nagashima[1] MD, Jun Nakayama[2] MD

[1]Department of Neurosurgery, Matsumoto, Japan, [2]Department of Laboratory Medicine, Shinshu University School of Medicine, Matsumoto, Japan

Summary Surgery was performed on the medulla oblongata of two adult patients with malignant glioma. Gross total resection of the tumors, located laterally or medially in the upper half of the medulla respectively, was achieved. The patient with the medially located tumor experienced significant postoperative neurological deterioration including sleep apnea. The other patient with the laterally located tumor showed symptomatic improvement without respiratory complications. The patient with an anaplastic astrocytoma survived approximately 4 years and the patient with a glioblastoma multiforme approximately 2 years. Although the upper half of the medulla is more critical than the lower half, a lateral approach to the upper half of the medulla appears to be relatively safer than a medial approach. Some cases of focal malignant gliomas in the medulla may be amenable to gross total resection in order to achieve improved outcome. Surgery can be undertaken when a tumor is unilateral and its margin appears relatively clear on magnetic resonance images.

Journal of Clinical Neuroscience (2004) 11(1), 75–80
0967-5868/$ - see front matter © 2003 Elsevier Ltd. All rights reserved.
doi:10.1016/j.jocn.2003.02.007

Keywords: brainstem, medulla oblongata, malignant glioma, surgical anatomy, direct surgery, surgery

Received 30 July 2002
Accepted 5 February 2003

Correspondence to: Dr. Kazuhiko Kyoshima MD, Department of Neurosurgery, Shinshu University School of Medicine, Asahi 3-1-1, Matsumoto 390-8621, Japan. Tel.: +1-81-26337-2688; Fax: +1-81-263-37-0480; E-mail: kakyosh@hsp.md.shinshu-u.ac.jp

INTRODUCTION

Intra-axial brainstem lesions can now usually be treated more safely than before due to recent improvements in neuroradiological and intraoperative technologies.[1–8] However, direct surgery on the medulla oblongata is still potentially hazardous due to the fact that the medulla oblongata contains the autonomic centers of most important vital functions. Damage to these structures is likely to result in significant morbidity and mortality. Certain subgroups of brainstem gliomas, mainly in paediatric patients, have recently been treated successfully by aggressive surgical intervention.[1,3–5,9–26] However, malignant brainstem gliomas are

generally considered to be inoperable, because their prognosis is so poor and not improved by surgical intervention, even radical removal.[5,11,12,19,20,26] Very few paediatric cases of malignant gliomas of the medulla oblongata that were subjected to radical resection with poor outcome, have been reported.[12,27] This report concerns 2 adult patients that underwent gross total removal.

MATERIALS AND METHODS

Case 1

A 42-year-old man presented with a 2-year history of hoarseness of voice was admitted. He had a 3 month history of nausea and dizziness followed by swallowing difficulty. On admission, he complained of hiccups. Neurological examination revealed a mild left facial and left lower cranial nerve paresis. This was manifested by sternocleidomastoid muscle weakness, loss of gag reflex, uvula deviation, curtain sign, hoarseness of voice, difficulty in swallowing and tongue deviation with muscle atrophy. In addition he had left cerebellar signs with gait disturbance and nystagmus. Preoperative magnetic resonance (MR) imaging revealed a heterogeneously enhancing tumor with a cystic component in the left side of the medulla oblongata (Fig. 1, upper).

Via a suboccipital craniectomy with C1 laminectomy, the medulla oblongata was exposed with minimal splitting of the vermis. The medulla oblongata was seen to bulge on the left side due to a tumor located just beneath the medullary surface (Fig. 2, left). A medullary incision was made approximately 8 mm lateral to the median sulcus of the fourth ventricular floor and the critical medial side was first dissected by retracting the tumor laterally with a two-pronged hook after aspiration of the cyst fluid. The tumor was then removed together with overlying brainstem tissue (Fig. 2, right). The resection margin obtained was relatively clear and the emerging zones of the lower cranial

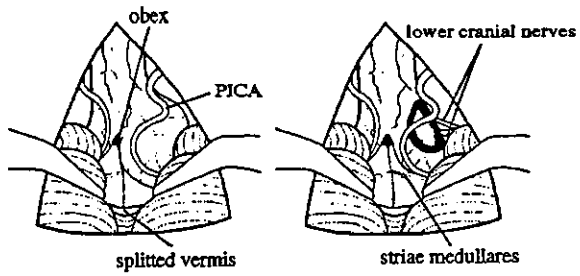

Fig. 2 Intraoperative schematic drawing via a suboccipital approach with the patient in the prone position (case 1). Left: the tumour is located intra-axially in the lateral part of the upper half of the medulla oblongata. Right: A macroscopic total resection of the tumuor including the overlying medullary tissue was achieved. PICA = posterior inferior cerebellar artery.

nerves were not affected by the tumor-the vital signs and somatosensory evoked potentials did not show marked change intraoperatively.

Postoperatively, the patient showed temporary worsening of his swallowing disturbance requiring a tracheostomy for 3 months. All sensory modalities remained intact and the symptoms and signs gradually improved. Histopathology revealed an anaplastic astrocytoma (astrocytoma grade 3) (Fig. 3, left). Postoperative MR imaging showed no residual tumor. After subsequent adjuvant irradiation and chemotherapy the patient was discharged with residual hoarseness of voice but without any compromise in his activities of daily living allowing him to return to work. Follow-up MR imaging 2 years and 3 months postoperatively revealed no tumor recurrence (Fig. 1, middle). However, MR imaging 3 years and 5 months postoperatively revealed tumor recurrence at a site distant from the resection cavity (Fig. 1, lower) although the patient's neurological status had not altered. The patient died 3 years

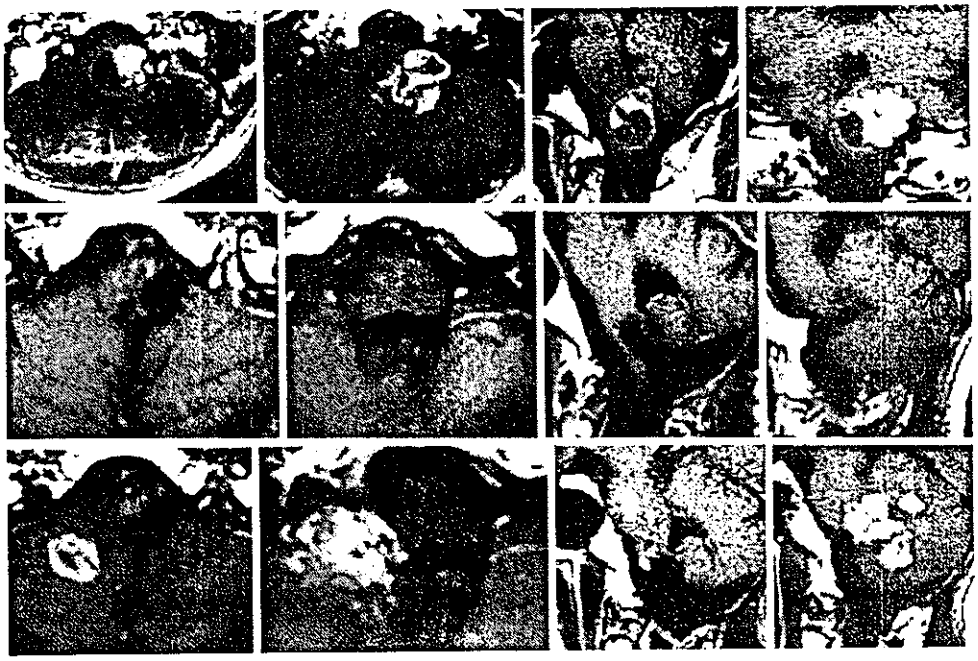

Fig. 1 Pre- and postoperative enhanced MR imaging (case 1). Upper: preoperative MR images revealing a heterogeneously enhanced cystic tumor with a relatively clear margin in the medulla oblongata on the left side. Middle: MR images 2 years and 3 months postoperatively showing no tumor recurrence. Lower: MR images 3 years and 5 months postoperatively showing tumor recurrence at a site distant from the tumor-removed cavity.

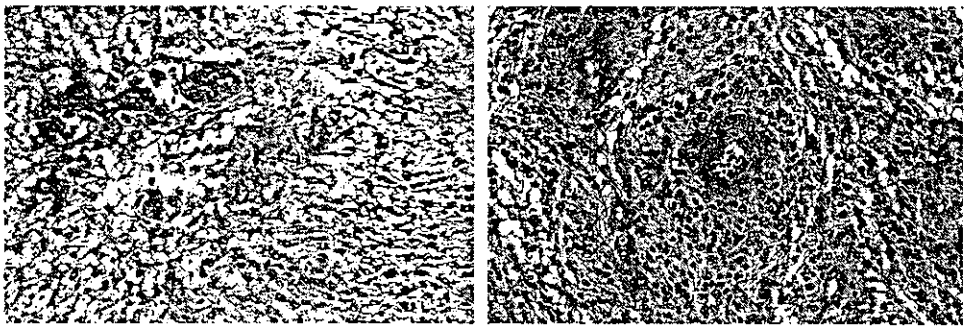

Fig. 3 Pathological findings (H&E). Original magnification 66×. Left (case 1): showing relative high cellularity of small spindle-shaped cells with vascular proliferation referred to as anaplastic astrocytoma (astrocytoma grade 3). Right (case 2): showing perivascular proliferation of round cells and their areas of high cellularity defined as glioblastomas; other specimens showing necrotic or hemorrhagic areas.

and 9 months postoperatively with reasonable quality of life until the final 4 months.

Case 2

A 55-year-old man with a 10-month history of voice hoarseness had been complaining of a progressive 2 month history of hiccups, vomiting, unsteady gait, difficulty in swallowing and clumsiness of the left hand. An MR image taken at another hospital one month before admission revealed a mass in the medulla oblongata.

On examination the patient had hypoalgesia of the right side of the face and slight bilateral hearing disturbance predominantly on the left hand side. The left lower cranial nerves palsy was manifested by uvular deviation, curtain sign, vocal cord palsy with a normal gag reflex, hoarseness and difficulty swallowing. He also had left cerebellar signs. Preoperative MR imaging revealed an enhancing mass with a relatively unclear margin in the left side of the medulla oblongata (Fig. 4, upper). Nine days prior to surgery he underwent a tracheostomy due to progressive difficulty with swallowing and frequent aspiration pneumonia.

Via a suboccipital craniectomy with C1 laminectomy the medulla oblongata was exposed without splitting the vermis. The tumor protruded from the floor of the fourth ventricle at the level of the medulla oblongata on the left (Fig. 5, left). The medial side of the tumor was first dissected from the floor. The tumor was then dissected from the surrounding brain tissue circumferentially. A dissection plane was then identified based on the colour and

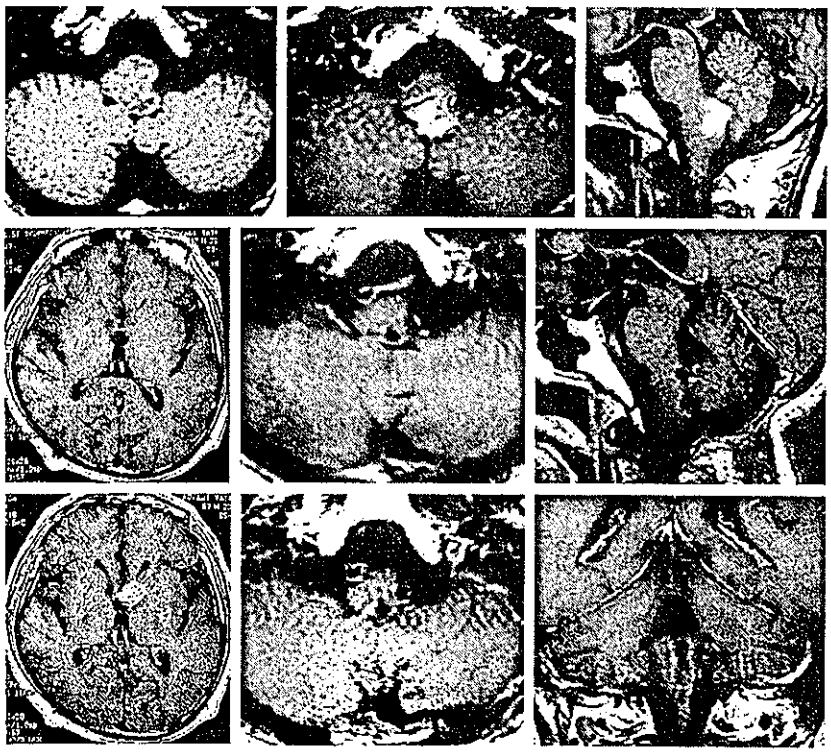

Fig. 4 Pre- and postoperative enhanced MR imaging (case 2). Upper: preoperative MR images revealing a well-enhanced mass with an irregular and relatively unclear margin in the medulla oblongata on the left side. The image shown on the *left* is not enhanced. Middle: MR images 1 year and 2 months postoperatively showing no tumor recurrence. Lower: MR images 1 year and 8 months postoperatively showing a disseminated tumor in the third ventricle without tumor recurrence in the original area.

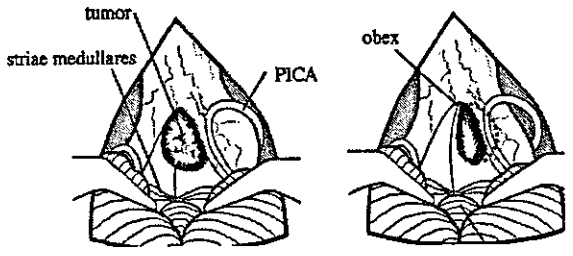

Fig. 5 Intraoperative schematic drawing (case 2). Left: The tumor protrudes from the floor of the fourth ventricle, and its intra-axial part is situated in the medial part of the upper half of the medulla oblongata. Right: Macroscopically, a total resection of the tumor was achieved. PICA = posterior inferior cerebellar artery.

hardness of the tumor and extended deeper. Care was taken not to retract the surrounding brain tissue. The main mass, located under medullary tissue, was undermined with a retraction-dissection method using a small spoon retractor. The intra-axial part of the tumor, where the tumor margin was relatively clear, was finally removed resulting in resection of the vagal and greater part of the hypoglossal triangles (Fig. 5, right). Intraoperatively, the patient experienced an episode of hypertension and reduced response of somatosensory evoked potentials. Transient disappearance of potentials was observed several times but they recovered by pausing the surgical procedure.

Postoperatively, the patient's swallowing difficulty deteriorated with ataxic gait, loss of gag reflex bilaterally, deterioration of hypoglossal function and sleep apnea for the first two days. However, sensation was well preserved, and even though, the hypoglossal nucleus had been almost completely removed, hypoglossal function was not totally compromised. Histopathology confirmed glioblastoma multiforme (Fig. 3, right). Postoperative MR imaging showed no tumor. Radiation therapy and chemotherapy were subsequently performed and a laryngectomy was performed 4 months later to treat severe swallowing disturbance. The patient was discharged with a tracheostomy and a gait disturbance persisted but he was able to walk with the aid of a stick. Oral intake was also possible and sleep apnea occurred occasionally. Follow-up MR imaging 1 year and 2 months postoperatively showed no tumor recurrence (Fig. 4, middle). However, 1 year and 8 months postoperatively, MR imaging revealed tumor recurrence in the third ventricle (Fig. 4, lower). This was irradiated with an X-knife. The patient died 2 years and 3 months postoperatively. His neurological condition remained stable until 1 year and 10 months postoperatively.

RESULTS

We achieved gross total removal of malignant gliomas in the medulla oblongata in two adults using an operating microscope. We did not use a laser or a Cavitron ultrasonic surgical aspirator. Patient 1 had an intrinsic (intra-axial) anaplastic astrocytoma located laterally in the upper half of the medulla oblongata and patient 2 had an exophytic glioblastoma, the main component of which was located medially within the upper medulla oblongata (Figs. 2, 5 and 6, right). Postoperatively, patient 1 showed symptomatic improvement but temporary worsening of dysphagia, while patient 2 showed neurological worsening and remained severely dysphagic with gait difficulties and sleep apnea. The postoperative survival of the patient with the anaplastic astrocytoma was 3 years and 9 months and the patient with the glioblastoma multiforme 2 years and 3 months. The recurrence-free period, based on MR imaging was at least 27 months for patient 1 and 14 months for patient 2. The recurrent masses were first noted at sites distant from the initial tumour location. The tumours progressed rapidly after recurrence and patients 1 and 2 both died 4 and 7 months later respectively. Patient 2 showed intraoperative disruption of somatosensory evoked potentials but no marked postoperative sensory impairment. The tumor tissue was distinguishable from adjacent brain tissue by its gray appearance and a distinct dissection plane defining the tumor borders was noted.

DISCUSSION

Brainstem gliomas are less common in adults than in children and their prognosis is generally poor. The majority of brainstem gliomas in both adults and children, arise predominantly in the pons and less often in the medulla oblongata.[14,18,28–32] Although some patients have a better prognosis and survive for more than several years,[9,11,13,16,30,33–38] for the majority of patients the prognosis is generally poor.[9,16,24,29,34,36,39–43] Such patients rarely survive more than 2 years after diagnosis.[3,9–11,13,16,18,21,34,36,38,42,44,45] Previously, brainstem gliomas were considered inoperable because of their infiltrative behavior and critical location. Recently, however, many authors have emphasized that some subgroups, such as dorsally exophytic or surface brainstem gliomas,[10,13,15,16,18–20,22,23] and focal intrinsic gliomas,[1,12] especially of the cervicomedullary junction[3–5] and the midbrain[15,23,25] are amenable to surgical re-

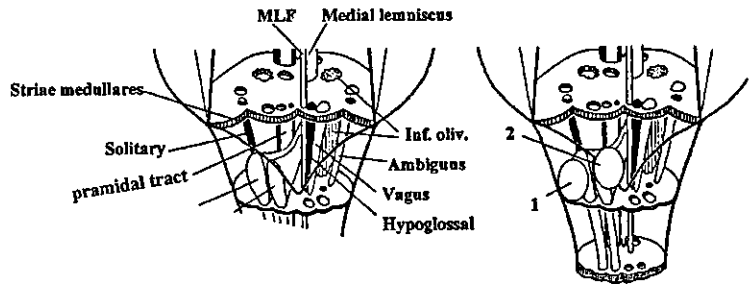

Fig. 6 Surgical anatomy and tumor location. Left: showing schematic 3-dimensional topography of internal structures of the medulla oblongata from a dorsal view. Note that important neural structures are densely located in the upper half of the medulla oblongata. The striae medullares run across the floor of the fourth ventricle roughly bordering the pons and medulla oblongata. The dorsal vagal and hypoglossal nuclei are situated under the posterior surface near the midline, the nucleus of the solitary tract is located anterolaterally to the dorsal vagal nucleus, the ambiguous nucleus is located further anterolaterally to the nucleus of the solitary tract, and the inferior olivary nucleus is located posterolaterally to the pyramidal tract and laterally to the medial lemniscus as well as anteromedially to the ambiguous nucleus. Ambiguus = nucleus ambiguus (ambiguous nucleus), cuneatus = nucleus cuneatus, gracilis = nucleus gracilis, hypoglossal = nucleus of the hypoglossal nerve (hypoglossal nucleus), inf. oliv. = inferior olivary nucleus, MLF = medial longitudinal fascicle, solitary = nucleus of solitary tract, vagus = dorsal nucleus of the vagus nerve (dorsal vagal nucleus). Right: showing tumor location in the upper half of the medulla oblongata in cases 1 and 2.